ICAS PAPER No. 72 - 33

SOME RESULTS FROM TESTS IN THE NAE HIGH REYNOLDS NUMBER TWO-DIMENSIONAL TEST FACILITY ON "SHOCKLESS" AND OTHER AIRFOILS

by
Lars H. Ohman, J. J. Kacprzynski and
D. Brown, Research Officers
National Research Council of Canada
Ottawa, Ont., Canada

The Eighth Congress of the International Council of the Aeronautical Sciences

INTERNATIONAAL CONGRESCENTRUM RAI-AMSTERDAM, THE NETHERLANDS
AUGUST 28 TO SEPTEMBER 2, 1972

Price: 3. Dfl.

SOME RESULTS FROM TESTS IN THE NAE HIGH REYNOLDS NUMBER TWO-DIMENSIONAL TEST FACILITY ON "SHOCKLESS" AND OTHER AIRFOILS

L.H. Ohman, J.J. Kacprzynski, D. Brown
National Research Council of Canada
Ottawa, Canada

Abstract

Results from investigations in the NAE high Reynolds number two-dimensional test facility on two classical NACA airfoils and two contemporary supercritical airfoils have been presented. The results have been compared with other published experimental data. Comparisons have also been made with results from theoretical calculations performed at NAE for subcritical as well as supercritical flow, incorporating boundary layer displacement effects for some subcritical cases. Experimental and theoretical results have compared favourably.

The comparisons with other experimental data have demonstrated good correspondence in some cases as well as gross discrepancies in other cases. For the latter, the discrepancies have been attributed to Reynolds number effects or differences in experimental techniques.

I. Introduction

In recent years there has been a strong resurgence of the interest in the development of airfoil sections for high subsonic and transonic speed as well as in determining more fully the aerodynamic characteristics of standard airfoils at these speeds and particularly examining the influence of Reynolds number.

This renewed interest in high speed (or transonic) characteristics of airfoils has, by necessity, brought with it the development of new test facilities as well as of more advanced theories.

One such new development is the high Reynolds number two-dimensional test facility at the National Aeronautical Establishment in Ottawa. This facility was commissioned in late 1969 and has since been in frequent use not only by NAE but also major aircraft companies and other research organisations.

Many types of airfoils have been investigated, some rather conventional and others of contemporary design. It is the purpose of this paper to present some of the more interesting and open results from these investigations, which will include not only the aerodynamic characteristics of the airfoils themselves but also results related to problems particular to two-dimensional testing, where wall interference is of much more concern than in three dimensional tests.

Since the facility has been fully described in other publications[1,2], only a brief description will be provided for the sake of completeness, including some new features which have added to its usefulness.

II. Brief Facility Description

The NAE 5 ft x 5 ft blowdown wind tunnel[3] has an air storage capacity of 50,000 cu.ft at 21.2 atm and 21°C. The wind tunnel shell structure is designed for 17 atm internal pressure. These are two main factors that limit the potential Reynolds number performance of this wind tunnel. Because of running time limitations the 5 ft x 5 ft test section can only be operated at a fraction of the maximum allowable pressure, but by using a reduced test section area operation at higher pressure is possible. In order to take full advantage of the capabilities thus offered to produce high Reynolds number for two-dimensional tests, the 15" x 60" test section (the "2D insert") was constructed, which can be assembled in the 5 ft x 5 ft transonic test section of the wind tunnel, see Figs. 1 and 2. The Reynolds number performance achieved through this arrangement is depicted in Fig. 3. At high subsonic Mach numbers a Reynolds number of 40×10^6 is possible for a 1 ft chord model, as compared with 15×10^6 in the 5 ft test section for about 10 seconds run time. In the 2D insert design special attention was paid to the control of the sidewall boundary layer[4]. Boundary layer bleed slots are located at the 2D inlet contraction to remove the rather thick boundary layer from the 5 ft tunnel sidewalls (the upstream 5 ft x 5 ft parallel section is about 45 ft long). Around the model location the sidewalls are made of porous material allowing distributed suction, as indicated in Fig. 1. This system has proved very effective in promoting two-dimensional flow over the full span of the model -- the adverse effect of the sidewall boundary layer is effectively eliminated in this way. The amount of air removed through sidewall suction is relatively small, ½ to 1% of the tunnel mass flow has proved sufficient in most cases. Because of the method of suction, the "sucked away" air is bled to atmosphere, a performance limit is imposed as indicated in Fig. 3. The curves labelled relative suction velocity represent the maximum amount of suction available for given combinations of Mach

number and Reynolds number.

Normally the top and bottom walls of the test section have 20.5% porosity (17 rows of ½" straight holes at 1.04" spacing). However, the porosity can easily be reduced by covering rows of holes with streamwise metallic strips and the facility has been operated at 6% porosity.

The model is supported on two 3-component balances which rotate with the model. With the recent installation of a modern data system it is now possible to use a fast scanning pressure measuring system and a fast traversing sidewall mounted wake rake system (see Fig. 1). Simultaneous force, wing pressure and wake traverse measurements are now made. The pressure measuring system allows the scanning of 80 surface pressures and a full wake survey in 2.5 seconds.

In order to eliminate the decay of Mach number during high pressure runs, caused by the adiabatic heating of the air in the wind tunnel in the starting process[1,2], a Mach number control system has been installed. The basis of this is a hydraulically operated servo-controlled flap in the diffuser throat, which is governed by the test section static pressure. This system is capable of holding the test Mach number constant to within ±0.001 during a run.

III. Quality of Wind Tunnel Flow

The 2D insert has been calibrated at both 20.5% and 6% porosity by taking pressure measurements on a centre line probe and the sidewall centre line. In addition some boundary layer measurements have been performed. For reasons later explained it is preferred to operate with the 20.5% porosity and calibration data relevant to this configuration only are presented. Results from calibration of the 6% porosity configuration are given in[5].

Fig. 4 shows the centre line Mach number distributions in terms of Mach number difference between the local Mach number and a reference Mach number as measured on the sidewall centre line. The figure covers a Mach number range from M = 0.55 to M = 0.92 at constant stagnation pressure. There is no appreciable pressure gradient along the whole parallel section of the wind tunnel. With increasing Mach number, however, a slight difference develops between the sidewall and the centre line distribution and the data also show larger scatter near the test section centre line. This situation is probably promoted by imperfections in the flatness of the porous sidewall panels[6]. The effect of sidewall suction is small but noticeable as exemplified in Fig. 5. There is a slight positive pressure gradient in the region influenced by suction. This gradient may be significant enough to influence the drag as measured by the sidewall balances. The displacement thickness of the sidewall boundary layer as determined by measurements with a traversing pitot probe just downstream of the porous panel[2,5] with no suction applied is 0.1" for test conditions corresponding to those in Fig.4. With a moderate amount of suction, say ½% of the tunnel mass flow, the thickness is reduced by about 50%.

From sound pressure measurements using a microphone mounted in the free stream just upstream of the 2D inlet the curves in Fig.6 have been derived. The overall sound pressure level in dB is plotted versus the pressure ratio across the control valve. The noise is primarily generated by the control valve, and it is seen that a pronounced peak occurs as the pressure ratio becomes critical. From these results it may be concluded that the turbulence level at the entrance of the 2D insert is between 0.4% and 0.8% which is further reduced, by a factor of about 5, to 0.1% to 0.16%, due to the 4 to 1 contraction ratio. However, the perforated top and bottom walls will obviously contribute to the turbulence level in the test section, but these contributions are primarily in the high frequency regime and are not expected to alter the above figure significantly. Because of the high turbulence level it has been the practice to perform tests with natural transition only.

Some flow angularity has been observed. Measurements with a symmetrical airfoil have indicated about -0.3°[7].

IV. Results for Conventional Airfoils

NACA 64A410

An example of a classical airfoil section investigated in the 2D insert is the NACA 64A410 section. Two models of 10" and 15" chord and with 57 pressure holes along the centre chord were tested at Reynolds numbers varying from 8 to 36x 10^6. Both 20.5% and 6% wall porosity were used in these investigations, which have been documented in[5,6].

Some selected samples of data from these tests will be discussed below to demonstrate:

i) agreement in subcritical pressure distribution between NAE and classical NACA experiments[8].
ii) correspondence in subcritical pressure distribution between 10" and 15" chord models at NAE.
iii) viscous effects on calculated pressure distributions in comparison with experimental data.
iv) discrepancies between NAE and NACA section coefficient data.

v) Reynolds number effects on supercritical pressure distributions, NAE vs NACA data.
vi) correspondence between calculated and experimental supercritical pressure distributions.

A typical example of the agreement in subcritical pressure distribution is shown in Fig.7. The two test conditions are not fully identical, the differences being in Reynolds number, chord to height ratio and geometric aspect ratio. Furthermore sidewall suction was applied in the NAE case. For this particular condition of subcritical flow and a moderate lift coefficient none of these differences, except possibly the sidewall suction is considered to be of significance.

Good correspondence in subcritical pressure distribution for the two NAE models is displayed in Fig.8. The slight difference in the character of the pressure distribution on the forward upper surface is attributed to profile errors which are rather large on the 10" model. The generally good agreement in data displayed in Figs. 7 and 8 indicates that for these types of conditions, interference effects from the top and bottom walls on the character of the pressure distributions are negligible.

Viscous effects on calculated pressure distributions are displayed in Fig.9. The theoretical pressure distributions are in both cases computed for the same C_N as the experimentally determined one used for the comparison. It is seen that including viscous effects is important in these types of calculations, even at this high Reynolds number, and considerably improves the agreement between calculated and measured data. The inviscid flow calculations were done using relaxation methods for solving the exact potential flow equations. The viscous flow calculations were performed in an approximate way using a method similar to the Lock-Powell-Sells-Wilby scheme[9-11].

Noticeable discrepancies between NAE and NACA section coefficient data are displayed in Fig.10. In the C_{N_α} vs M graph, the broad band representing NAE data was obtained using the 10" and 15" models at both 6% and 20.5% porosity and applying appropriate wall corrections [12,2]. The difference in C_{N_α} at the highest Mach number is probably due to the large difference in Reynolds number between the NACA and NAE data. Here the flow is supercritical and Reynolds number can be expected to have significant influence. At the lower Mach numbers, with subcritical flow, Reynolds number assumes a less important role and there is good agreement. A more significant difference between NAE and NACA data is displayed in the upper part of Fig.10, showing C_m versus C_N. The thick band comprises NAE data as obtained on both models from pressure integration as well as sidewall balance measurements and at the 6% and 20.5% wall porosities. The NACA data were obtained from sidewall balance measurements[8]. Although it cannot be conclusively demonstrated, it is believed that these rather large differences are due to differences in the experimental technique; the NAE tests being performed with sidewall boundary layer control while no corresponding control was applied in the NACA case.

Reynolds number effects are likely to be most pronounced in supercritical flow and in Fig.11 such a case is presented, where low Reynolds number NACA data are compared with high Reynolds number NAE data. The low Reynolds number data show a smooth pressure recovery over the upper surface, with some trailing edge separation. In the high Reynolds number case a strong shock occurs causing a more pronounced flow separation.

Good correspondence between calculated and experimental pressure distributions for supercritical flow is demonstrated in Figs.12a and b. The cases chosen are a low Reynolds number, slightly supercritical case and a high Reynolds number, highly supercritical case. The theoretical pressure distributions were obtained by inviscid potential flow calculations using relaxation methods according to a procedure recently developed at NAE by Kacprzynski[13]. The good agreement in the shock region is quite remarkable. It should be noted that while the comparison is based on "same C_N" there is a difference in incidence. The theoretical incidence is 0^c while the uncorrected incidence in the wind tunnel is 2^c and 2.4^c respectively. Estimated wall corrections and flow angularity may amount to about -1^c, which leaves a significant difference that cannot be accounted for.

NACA 65_1-213

One of the airfoil sections investigated at NAE, for which it has been possible to find comparable flight test data, is the NACA 65_1-213 section. The flight tests[14,15] which included pressure and accelerometer measurements were conducted on a Lockheed F80 aircraft, which is basically a straight wing configuration. The pressure measurements referred to in the following were taken on the inner "clean" position of the wing and the accelerometers, mounted near the aircraft CG, were used as buffet detectors.

The NAE data were obtained for a 15" chord model with the 2D insert top and bottom walls at 20.5% porosity. The investigation was carried out at Reynolds numbers as high as 45×10^6. In Figs.

13a and b the pressure distributions from flight and wind tunnel are compared under nearly identical values of Mach number, Reynolds number and normal force coefficient.

Fig.13a is for a slightly supercritical case at M = .71 while Fig.13b is for a highly supercritical case at M =.75. The pressure distributions are in fairly good agreement. Naturally the flight test data show more irregularities since some aeroelastic deformation of the airfoil shape in flight can be expected. It is remarkable, that in spite of this the agreement in the shock region is so good for the M = .75 case, Fig.13b.

A comparison of buffet boundaries given in Fig.14 show very good correspondence between wind tunnel and flight. The flight test data were determined from accelerometer readings[15] while the NAE data are based on observing the divergence of the pressure on the upper surface near the trailing edge, x/c = 0.95, applying the criterion $\partial C_p/\partial C_N = -0.4$. This criterion has been chosen in the absence of a well defined break in the pressure incidence history. Although it may seem rather arbitrary, it is based on correspondence observed with buffet onset as indicated by the sidewall balance for several other airfoils. The comparison is for a Reynolds number of 17×10^6. As mentioned, the NAE investigation was carried to a Reynolds number of 45×10^6 and it is seen in the right hand part of Fig.14 that there is a slight increase in the buffet onset velocity at this highest Reynolds number, but not much change for Reynolds numbers from 17×10^6 to 35×10^6.

The upper part of Fig.14 shows typical histories for the trailing edge pressure at $R_e = 17 \times 10^6$ indicating the points of buffet onset. It should be noted that buffet occurs well before $C_{N_{max}}$ for this airfoil.

V. Results for Modern Airfoils

As an example of research on contemporary airfoils at NAE, some results on the NLR shockless symmetrical airfoil 011-0.75-1.375[16] and the Garabedian-Korn shockless lifting airfoil [17,18] are presented. The NLR symmetrical airfoil is an 11.6% thick quasi-elliptical section with a theoretical design Mach number of $M_D = 0.78612$. Results from NLR tests on this section are reported in[19] and some of those results will be referred to in the following.

The 10" NAE model has 60 pressure holes along the centre chord with 49 located on the "upper" surface. A comparison of theoretical and actual model dimensions is given in Fig.15. Corresponding data for the forward part of the NLR model of the same section are also depicted in the figure, demonstrating very similar degree of accuracy in the contour of the two models.

Some representative results obtained at NAE at a Reynolds number of 21×10^6 are given in Figs.16 to 20. A typical subcritical case is presented in Fig.16 giving the pressure distribution near zero lift in comparison with inviscid theoretical results. The C_N value ($C_N = -0.011$) is derived from balance measurements (insufficient number of pressure holes on the lower surface does not permit accurate pressure integration for normal force) and has been used for the theoretical calculations. The general agreement is good although it does appear that the theoretical suction peak has not been fully realised in the experiment. A comparison with NLR results for the design case[19] is given in Fig.17. The NAE results were obtained in the same way as the NLR results. From a series of tests with small variations in Mach number and incidence those results that most closely agreed with the theoretical design curve were chosen to represent the design case. There are some notable differences between the two sets of data. The NLR results are in much closer agreement with the theoretical design curve, while the NAE results show definitely the existence of a weak shockwave at 20% chord. Nearer the leading edge the results are in very good agreement, and this latter would suggest that model discrepancies can be discounted when explaining the differences between the results. The differences can probably be attributed to Reynolds number effects. The sensitiveness of the pressure distribution, experimental as well as theoretical, in the shock region to small changes in the free stream parameters (M, α) is indicated in Fig.18. These results illustrate the difficulties one encounters in attempting experimentally to determine conditions for shock free flow.

A further comparison with NLR results is given in Fig.19 which shows the drag coefficient near zero lift as obtained from wake pressure measurements. The differences in data at Mach numbers below M_D is consistent with the difference in Reynolds number; above M_D the NAE and the NLR fixed transition data overlap while the NLR free transition drag values are somewhat lower.

A demonstration of the steadiness (or unsteadiness) of the flow for supercritical conditions is given in Fig.20. These results were obtained by performing several pressure scans during one wind tunnel run. There is noticeable unsteadiness of the pressure in the shock region and some minor fluctuations on the upstream part of the airfoil while downstream of the shock the flow exhibits a very stable character. The only plausible

conclusion to be drawn from this is that in supercritical flow the supersonic region is slightly unsteady.

It is worth noting that in both the NAE and NLR experiments the design Mach number was determined as $M_D = 0.789$, which is 0.003 higher than the theoretical value. The good agreement between the NLR and NAE results is quite remarkable when one considers the differences in the experimental arrangements and Reynolds numbers. At NLR slotted walls with 10% open area were used, model aspect ratio was 2.5, chord to height ratio 1 to 3.05 and sidewall boundary layer control was not applied. At NAE the perforated walls had an open area of 20.5%, the aspect ratio was 1.5, chord to height ratio 1 to 6 and sidewall boundary layer control was used. This good agreement is for practically shockless flow, where the interaction between the weak shock waves and the boundary layer is very small in both the high and the low Reynolds number cases. In off-design conditions, with strong shock waves, much larger effects of Reynolds number are to be expected.

A full account of the NAE investigation of this airfoil is given in[20].

The second example concerns the shockless lifting airfoil No.1 designed by Garabedian and Korn. Results from an earlier investigation of this airfoil were presented in[21,22]. The main purpose of the previous investigation was the verification of the Garabedian theory. The experimental part of the investigation was performed at 6% wall porosity, without automatic Mach number control and with a slow pressure scanning system. Although the reported results confirmed the theory, it was thought worthwhile to further investigate this airfoil and to see if better agreement in pressure distribution could be obtained in the modernised facility, in particular to find an explanation for the difference between the theoretical and experimental design Mach numbers 0.750 and 0.765 respectively. This second investigation included the determination of $C_{N_{max}}$ and buffet boundaries at various Mach numbers. The data from this investigation is fully reported on in[23]. For experimental design flow conditions improved agreement between experimental and theoretical pressure distributions is obtained, Fig. 21. In Fig.22 results from four consecutive pressure scans during one wind tunnel run are shown. Although the individual scans exhibit hardly any scatter in the results, as compared with the results from the earlier investigations, see Fig.21 for example, there are notable differences between the various scans in the shock wave region. These results are similar in character to those obtained with the shockless symmetrical airfoil (Fig.20). The fact that the recent results show much less scatter as compared with earlier results is attributed to the successful operation of the Mach number control system and a fast pressure scanning system in the recent investigation.

An interesting consequence of these variations of pressure in the recompression region has been investigated by Kacprzynski. He performed boundary layer calculations using the Nash-Macdonald method[24] with the measured pressure distributions representing the pressure field. The results of these calculations are plotted in Fig.23 which depicts the boundary layer displacement thickness over the chord of the airfoil, calculated for the pressure distributions corresponding to the four different pressure scans. The instability of the boundary layer near the shock wave and its correspondence with the observed pressure oscillations is quite obvious.

The maximum lift and buffeting characteristics were investigated over a limited Mach range $0.5<M<.77$ for a Reynolds number of 21×10^6. The results are summarised in Fig.24 which shows C_N vs α and buffet boundaries, both as determined from balance measurements. The character of the C_N versus α curves around $C_{N_{max}}$ is generally flat suggesting that this airfoil has gentle stalling characteristics at high Reynolds numbers. This is furthermore supported by the pitching moment results, which show only small variations with incidence, even in the stall-region, for the Mach numbers investigated.

Buffet condition was determined by observing the onset of oscillations for one of the downstream normal force elements of the sidewall balance. The onset of buffet was very gradual and a clear buffet onset condition was therefore difficult to determine. For $M<0.70$ pronounced buffet was observed well beyond $C_{N_{max}}$ with incipient buffet at about $C_{N_{max}}$. For the design Mach number, $M_D = 0.768$ pronounced buffet was observed at $C_{N_{max}}$ and incipient buffet at a slightly lower incidence. In the latter case the behaviour of the pressure versus incidence over the rear upper surface has been investigated. In Fig.25 the pressure coefficients for chord stations x/c = 0.95, 0.85, 0.75 and 0.65 have been plotted versus incidence. Good correspondence is demonstrated between pressure divergence at the 0.95 station and the occurrence of incipient buffet as indicated by the balance. An interesting phenomenon is the break in the pressure profile with incidence occurring at 3.8° which corresponds to the onset of pronounced buffet as sensed by the balance. No plausible explanation for this break in the pressure profile and its relation to buffet can be offered. It is worth noting that with the standard NACA 65_1-213 airfoil, previously discussed, buffeting occurred well before $C_{N_{max}}$ while this modern airfoil

is buffet free up to $C_{N_{max}}$, within the investigated Mach number range.

The drag coefficient as determined by wake pressure measurements is plotted versus Mach number for constant values of C_N in Fig.26. It shows the interesting feature that in the drag rise region, M>0.75, the airfoil drag is fairly insensitive to the value of C_N for $C_N \leq$ 0.65, actually more so than at M = 0.7. For comparison, drag values of the 10% thick NACA 64A410 section at C_N = 0.58 (the experimentally determined design value for the shockless airfoil) are shown. These clearly illustrate the advantage in drag that can be offered by a properly designed supercritical airfoil. It should be mentioned that the theoretical design Mach number for this airfoil is M_D = 0.750. The design Mach numbers determined experimentally are 0.765 and 0.768 for 6% and 20.5% wall porosity respectively. Theoretical direct calculation by Garabedian and independently by Kacprzynski confirms that the Mach number for shockless flow is M = 0.750. For the time being no well supported explanation for this discrepancy between theory and experiment can be offered. It is known that the wind tunnel model suffered from some significant profile errors[21,22] and this in combination with boundary layer displacement effects may be the main reason for this discrepancy.

VI. Some Problems Encountered in Two-Dimensional Investigations

It was mentioned in Section 3 that it is preferred to operate the facility at a porosity of 20.5%. The main reason for this is the result of a wall interference study by Mokry[12], which shows that the flow curvature effect due to wall interference is a minimum near this porosity. Although the correction to angle of attack will be larger at 20.5% than at 6% porosity, it is felt that this is to be preferred rather than having to introduce a somewhat uncertain correction due to flow curvature in addition to an angle of attack correction. Furthermore, the empty tunnel calibration data show a smoother character at the higher porosity. The wind tunnel can also be operated at a higher Mach number than in the low porosity case.

The main factor which adversely influences the two-dimensionality of the flow over the model is the interference between the model and the sidewall boundary layer. The need for minimising this interference is particularly important at transonic speed. The approach taken in the present facility with distributed suction has proved successful and evidence to that effect has been given in previous publications [2,6,25].

Fig.27 taken from[2], illustrates the effect of suction on the model surface flow for a supercritical case. Some recent data from simultaneous balance and pressure measurements (this possibility did not exist in earlier investigations) to further demonstrate that with adequate sidewall suction two-dimensional flow can be achieved for a variety of conditions is presented in Fig.28. This shows a direct comparison between the normal force coefficient obtained from balance measurements along the centre line of the model. The data presented in Fig.28 represent a variety of conditions for both the shockless lifting airfoil and the NACA 64A410 airfoil with adequate sidewall suction applied (V_n/V_∞ = 0.005 - 0.006). The agreement is generally very good, implying that two-dimensional conditions exists over the full span of the models. The points of high C_N for the shockless lifting airfoil, which show larger deviations, are for supercritical conditions with strong shock waves, where the shock induced boundary layer separation may destroy the two-dimensionality of the flow.

The equality of wake drags at various spanwise locations might be taken as another indication of two-dimensionality. However, results obtained at NAE have not provided very good evidence to that effect. The results presented in Fig.29 were obtained for the shockless lifting airfoil using the sting mounted wake probe described in[1]. Measurements were made at three different streamwise locations with the three pitot heads positioned as illustrated in the figure. The most downstream location corresponds to the position for the sidewall mounted wake rake. The results show that the drag level is not influenced by the streamwise position of the measuring station and that the spanwise variation in drag is consistent for the three streamwise stations. Bearing in mind that each set of three values represent one wind tunnel run it has to be concluded that the spread in drag values with spanwise position is genuine and not to be interpreted as scatter of data. These spanwise variations in drag could possibly be caused by variations in the transition position along the span, although at this high Reynolds number the expected variations are likely to be very small. Similar large spanwise variations in drag have been observed in two-dimensional tests at NPL[26], although at a much lower Reynolds number but with fixed transition. This raises some doubt as to the attainable accuracy of drag data from two dimensional tests. Drag data obtained by balance measurements generally do not agree with wake drag results. In Fig.29 the balance drag which is obtained by summing the balance chord and normal force components in the corrected free stream direction (corrected for flow angularity and wall

interference based on[2,7,12] has been included for comparison. No balance data have been given for the M = 0.8 case since wall corrections are not known for this Mach number.

The balance drag data show good repeatability but are consistently lower than the wake drag data by about 0.0025. This discrepancy could possibly be explained as a buoyancy effect due to the pressure gradient induced by sidewall suction. Applying the pressure gradient deduced from Fig.5 we obtain a buoyancy correction to the drag coefficient of -0.0020 which is close to the observed discrepancy. It should be noted that although the calibration data in Fig.5 are for a "typical" case, they do not truly represent any of the conditions in Fig.29. Whence the buoyancy effect can only be offered as a plausible but not conclusive explanation of the observed drag discrepancies.

VII. Conclusions

Results from investigations in the NAE high Reynolds number two-dimensional test facility on two classical NACA airfoils and two contemporary supercritical airfoils have been presented. The results have been compared with other published experimental data. Comparisons have also been made with results from theoretical calculations performed at NAE for subcritical as well as supercritical flow, incorporating boundary layer displacement effects for some subcritical cases. Experimental and theoretical results have compared favourably. The comparisons with other experimental data have demonstrated good correspondence in some cases as well as gross discrepancies in other cases.

The main conclusions to be drawn from the presented results are that:

i) for supercritical conditions Reynolds number effects on pressure distribution and section coefficients are significant.

ii) for supercritical conditions the flow in the supersonic region on shockless airfoils is slightly unsteady.

iii) shock wave position and buffet onset for a straight wing aircraft may be adequately predicted by high Reynolds number two-dimensional testing.

iv) adequate and economical numerical methods now exist for the calculation of both subcritical flow, including boundary layer displacement effects, and inviscid supercritical flow.

v) differences in experimental techniques may be the major cause for differences in experimental results from various sources, particularly for supercritical flow conditions; sidewall boundary layer control is desirable.

vi) wake pressure measurements offer the best known drag value. However, interpretation of drag results requires knowledge of transition position, for which no adequate method seems to be available for high Reynolds numbers.

vii) wall correction with regard to balance drag and stream direction for supercritical flow conditions remains an unsolved problem.

NOMENCLATURE

b	test section width, model span
H	test section height
c	model chord
C_N	normal force coefficient
C_m	pitching moment coefficient around 25% chord
C_{D_W}	drag coefficient from wake measurements
C_{D_B}	drag coefficient from balance measurements
C_p	pressure coefficient $\frac{p-p_\infty}{q_\infty}$
C_p^*	critical pressure coefficient
M	free stream Mach number
M_D	design Mach number
M_{Ref}	test section reference Mach number
ΔM	Mach number difference, $M(\text{local})-M_{Ref}$
p	local static pressure
p_∞	free stream static pressure
p_o	free stream stagnation pressure
q_∞	free stream dynamic pressure
R_e	Reynolds number based on airfoil chord
V_n	suction velocity = velocity component normal to porous sidewall
V_∞	free stream velocity
X	test section streamwise coordinate, model chordwise coordinate
Δy	difference in thickness coordinate between actual and theoretical model dimensions
α	incidence
α_g	geometric incidence = angle between airfoil chord and test section centreline
δ^*	boundary layer displacement thickness

REFERENCES

1. HSA STAFF, The NAE High Reynolds Number 15" x 60" two-dimensional test facility. Part I: General Information. NRC/NAE LTR-HA-4. Apr/70.

2. OHMAN, L.H., BROWN, D., The NAE High Reynolds Number 15" x 60" two-dimensional test facility: Description, Operating Experiences and some Representative Results. AIAA Paper No.71-293.

3. BROWN, D. Information for Users of the NRC 5 ft x 5 ft Blowdown Wind Tunnel at the NAE. Second Edition. NRC/NAE LTR-HA-6. Sept/70.

4. RAINBIRD, W.J., Design and use of boundary layer control for 2D aerofoil testing: NAE 15"x 60" section. NRC/NAE HSA-40. Feb/70.

5. BROWN, D., MOKRY, M., OHMAN, L.H. Calibration tests of the NAE high Reynolds number 15"x 60" 2D facility with 6% porosity. NRC/NAE Project Report 5x5/0050. Sept/71.

6. OHMAN, L.H., BROWN, D., The NAE high Reynolds number 15" x 60" two-dimensional test facility. Part II: Results of Initial Calibration. NRC/NAE LTR-HA-4. Sept/70.

7. KACPRZYNSKI,J.J., Analysis of the wind tunnel flow angularity and repeatability of test results in supercritical conditions. NRC/NAE HSA-55. Dec/71.

8. STIVERS, L.S., Effects of subsonic Mach numbers on the forces and pressure distribution of four NACA 64-A series airfoil sections at angles of attack as high as 28°. NACA T.N. 3162. 1954.

9. LOCK, R.C., POWELL, B.J., SELLS, C.C.L., WILBY, P.C. The prediction of airfoil pressure distribution for subcritical viscous flows. Transonic Aerodynamics, AGARD Conference Proceedings No.35, 1968.

10. KACPRZYNSKI,J.J., Fortran IV programme for the Sells method for subcritical two dimensional inviscid flow calculations past a lifting airfoil. NRC/NAE LTR-HA-3. Apr/70.

11. KACPRZYNSKI,J.J. Note on a method used in NAE for the subcritical viscous flow calculations past an airfoil. NRC/NAE HSA-53. Jul/71.

12. MOKRY, M., Higher-order theory of two-dimensional subsonic wall interference in a perforated wall wind tunnel. NRC/NAE LR-55. Oct/71.

13. KACPRZYNSKI,J.J. Exten of Sells' method to supercritical calculations. (To be published).

14. BROWN, H.H., CLOUSING, L.A., Wing pressure-distribution measurements up to 0.866 Mach number in flight on a jet-propelled airplane. NACA TN 1181. 1947.

15. GADEBURG, B.L., ZIFF, H.L., Flight determined buffet boundaries of ten airplanes and comparisons with five buffeting criteria. NACA RM A50I27. 1951.

16. BOERSTOEL, J.W., A survey of symmetrical transonic potential flow around quasi-elliptical airfoil sections. NLR TR T.136. 1967.

17. GARABEDIAN, P.R., KORN, D.G., Analysis of transonic airfoils. Comm. Pure & Appl.Math. Vol.24, 1971.

18. BAUER, F., GARABEDIAN, P.R., KORN, D.G. Supercritical Wing Sections. Springer Verlag 1972.

19. SPEE, B.M.,UIJLENHEOT, R., Experimental verification of shock-free transonic flow around quasi-elliptical airfoil sections. NLR MP 68003 U.

20. KACPRZYNSKI,J.J. Wind tunnel investigation of the Boerstoel shockless symmetrical airfoil 011-0.75-1.375. NRC/NAE Project Report 5x5/0061. 1972.

21. KACPRZYNSKI,J.J.,L.H.OHMAN.,Wind Tunnel tests of a shockless lifting airfoil.No.1. NRC/NAE Project Report 5x5/0054, 1972.

22. KACPRZYNSKI,J.J., OHMAN, L.H., GARABEDIAN, P.R., KORN, D., Analysis of the flow past a shockless lifting airfoil in design and off-design conditions. NRC/NAE LR-554. Nov/71.

23. KACPRZYNSKI,J.J., A second series of wind tunnel tests of shockless lifting airfoil No.1. NRC/NAE Project Report 5x5/0062.

24. NASH, J.F., MACDONALD, A.G.J., The calculations of momentum thickness in a turbulent boundary layer at Mach numbers up to unity. ARC - CP No.963. 1967.

25. PEAKE, D.J., YOSHIHARA, H., ZONARS,D. CARTER, W., The transonic performance of 2D jet-flapped aercfoils at high Reynolds numbers. AGARD Conference Proceedings 83-71. 1971.

26. THOMPSON, B.G.J., Carr-HILL, G.A. A programme of research into viscous aspects of flow on swept wings. NPL Aero Note 1100, Sept/70.

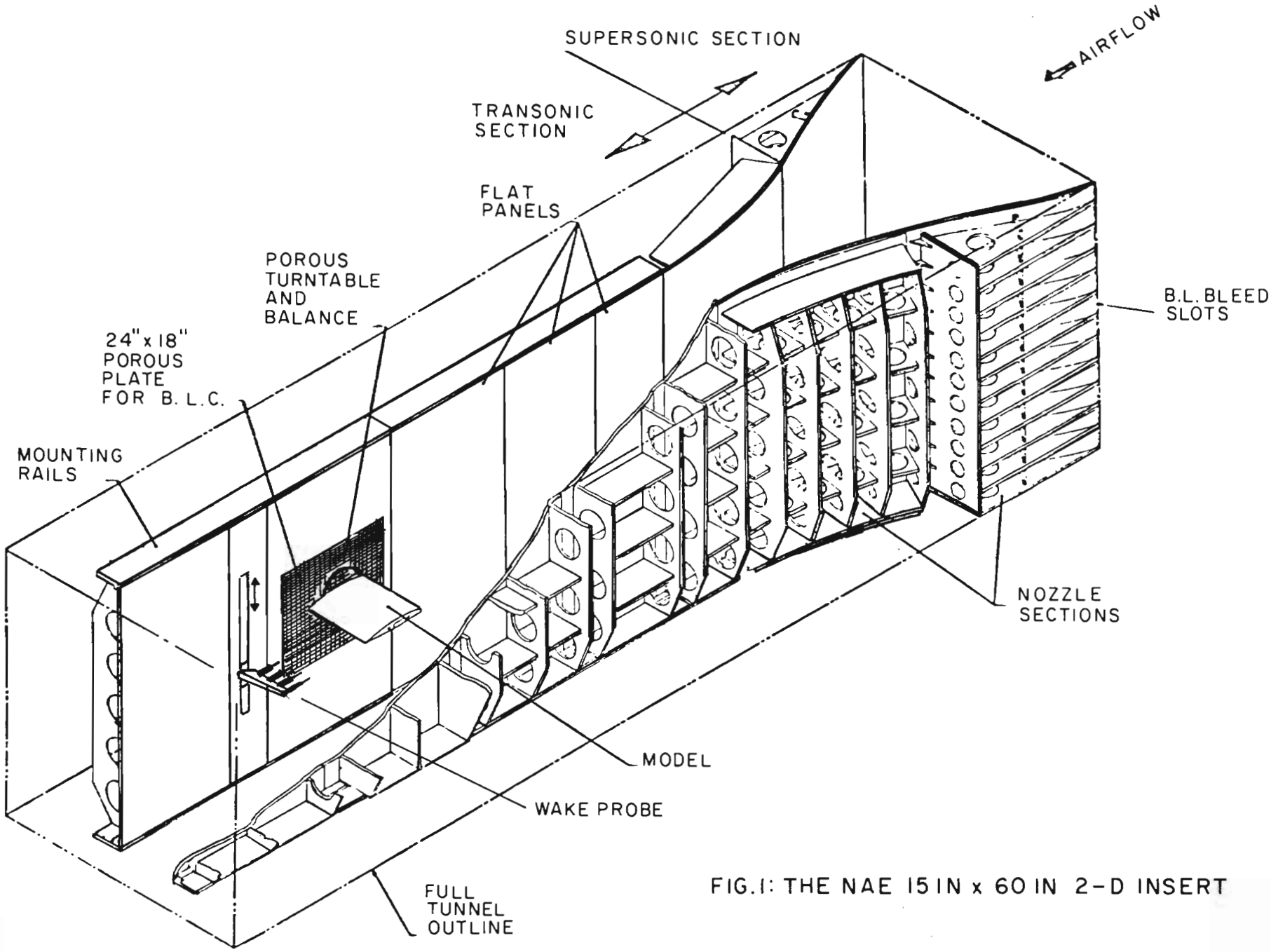

FIG.1: THE NAE 15 IN x 60 IN 2-D INSERT

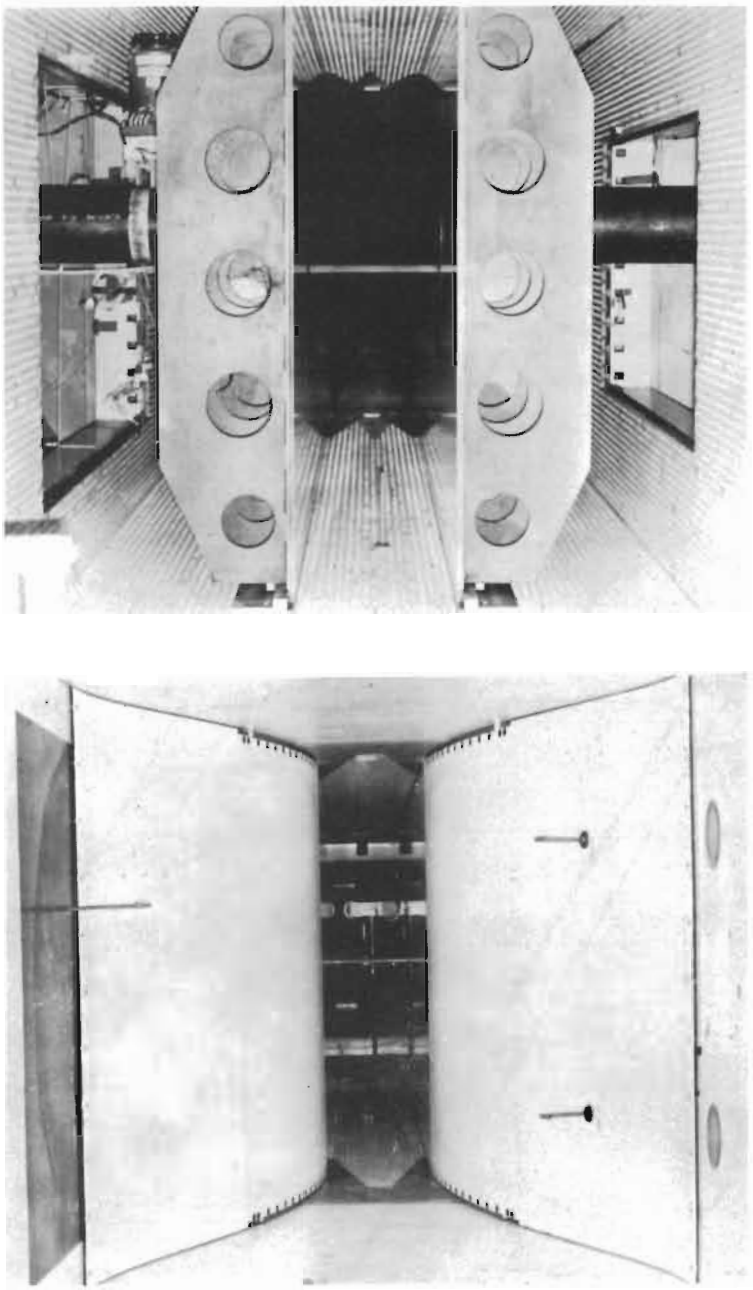

FIG.2: UPSTREAM AND DOWNSTREAM VIEW
OF 2-D INSERT

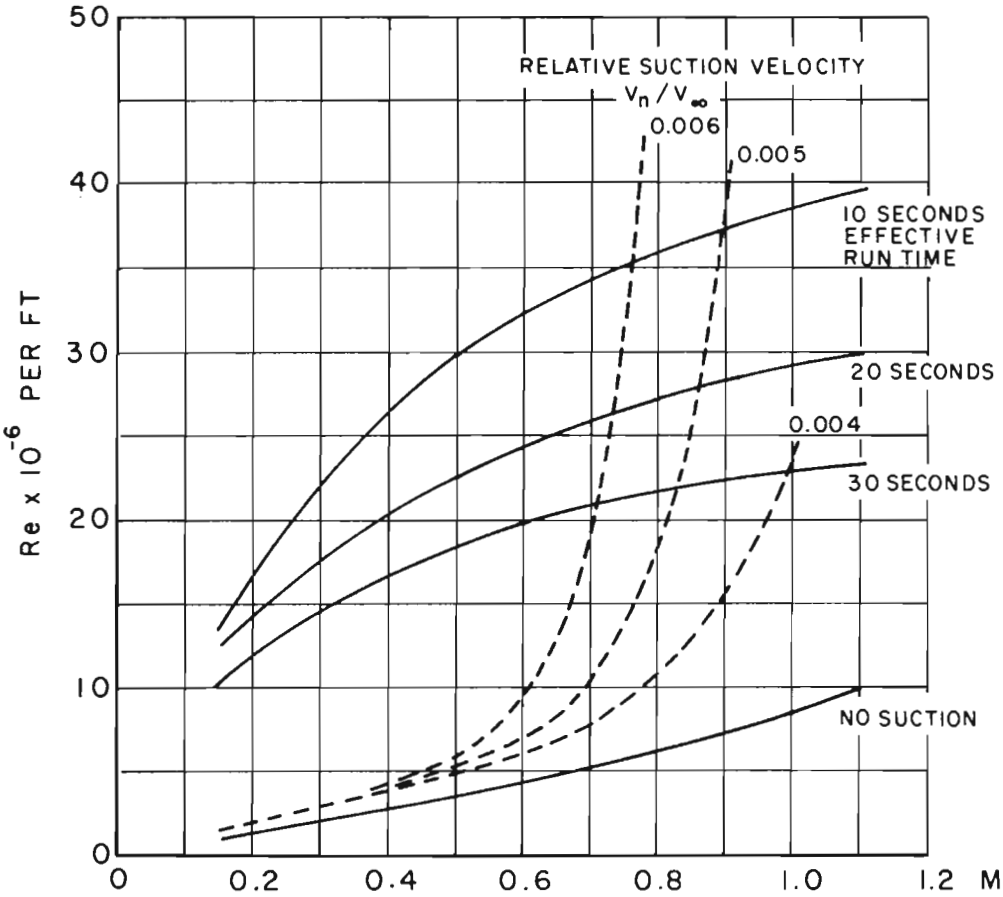

FIG. 3: PERFORMANCE OF THE NAE 2-D TEST FACILITY

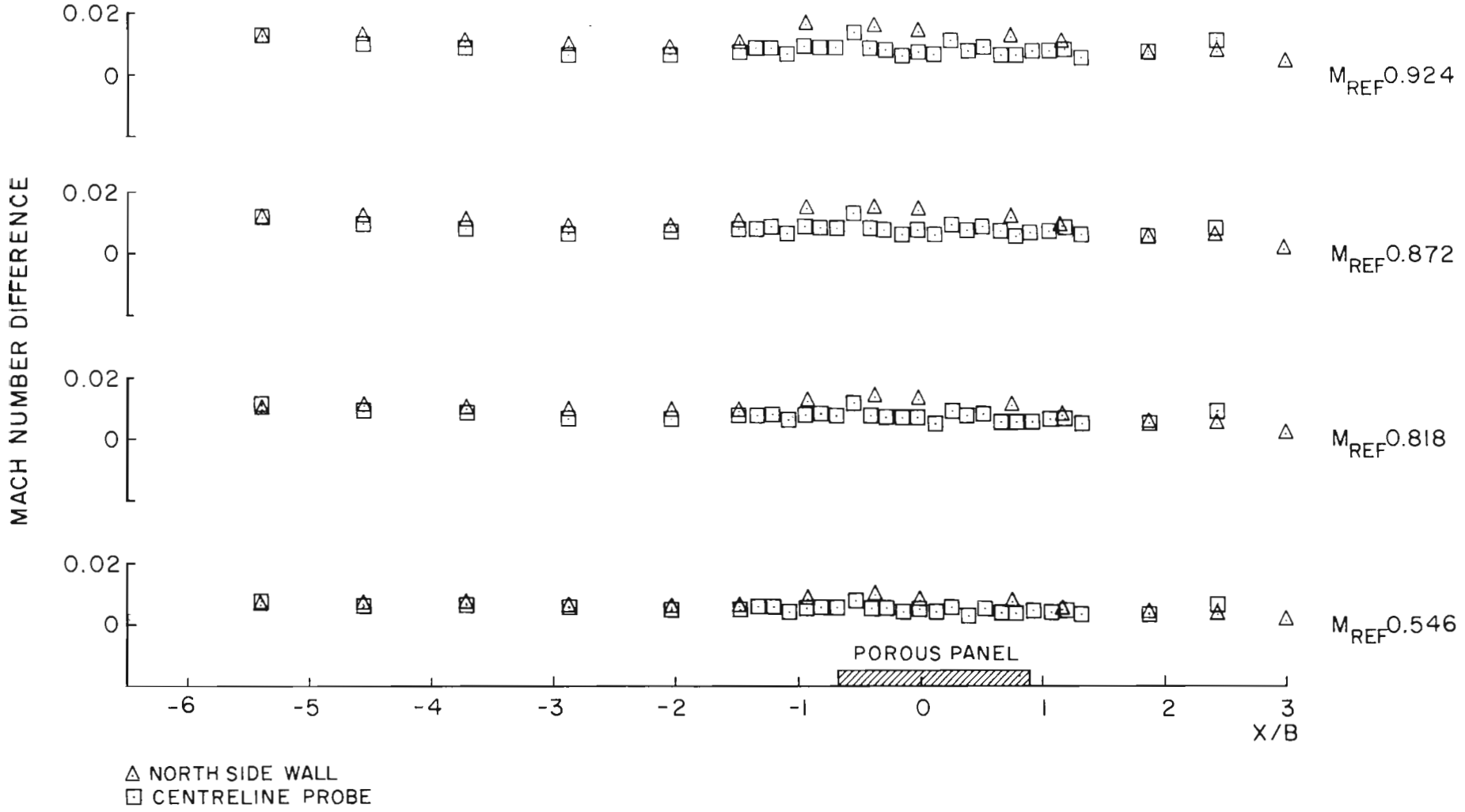

FIG.4: CENTRELINE MACH NUMBER DISTRIBUTION FOR P_0 = 6 ATM

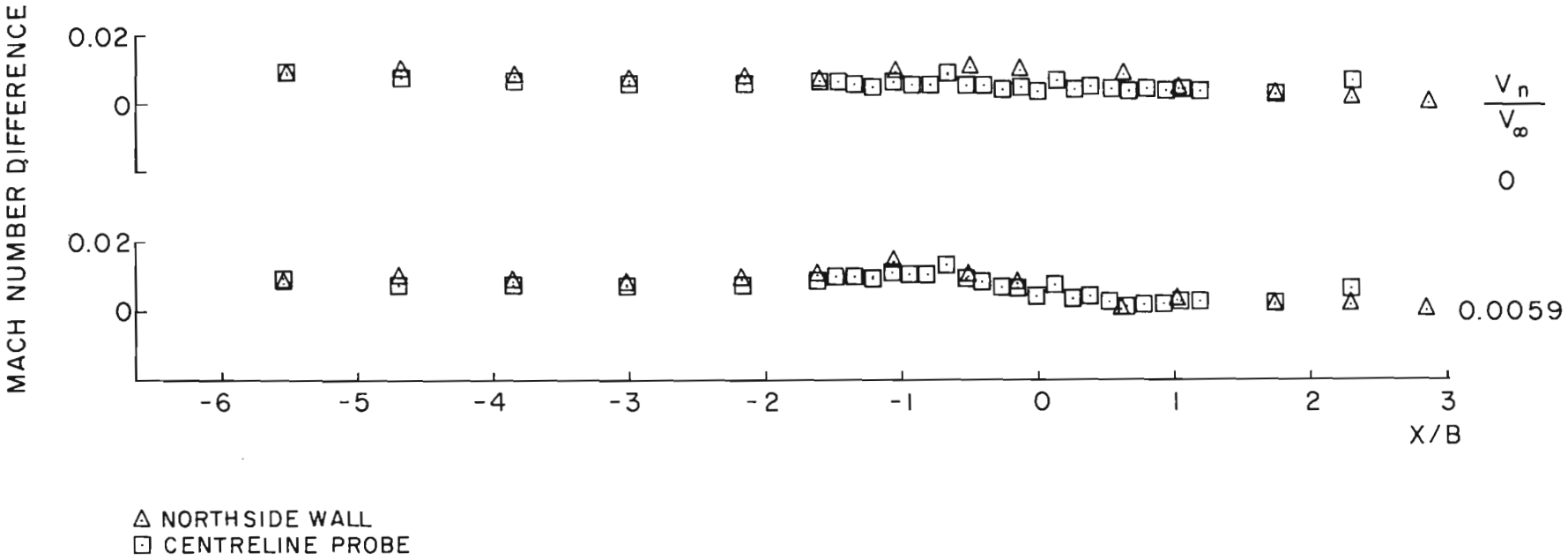

FIG. 5: EFFECT OF SIDEWALL SUCTION ON CENTRELINE MACH NUMBER DISTRIBUTION, $M = 0.70$, $P_0 = 6$ ATM

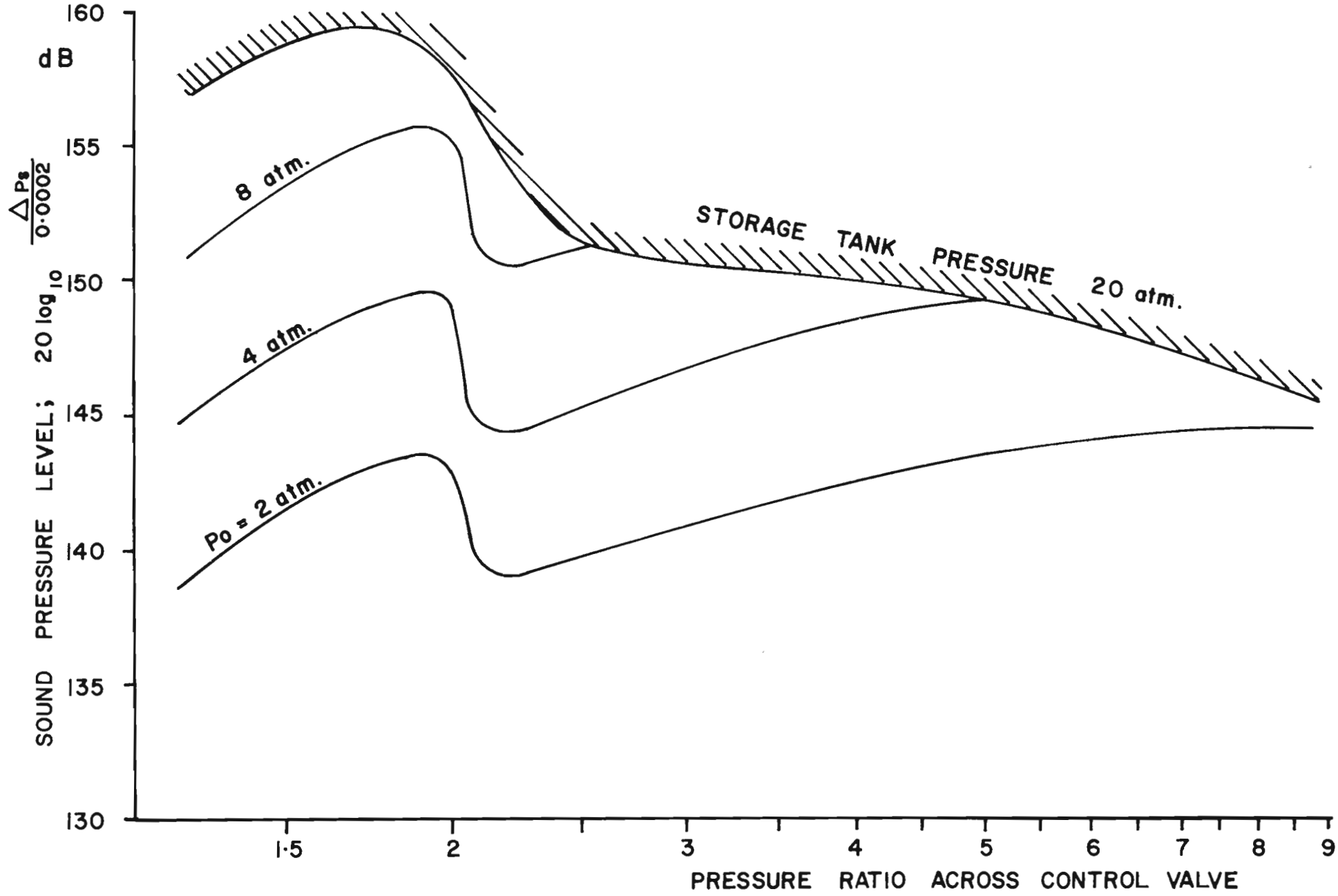

FIG 6: SOUND PRESSURE LEVEL AT ENTRANCE OF 2-D INSERT FOR M = 0.7

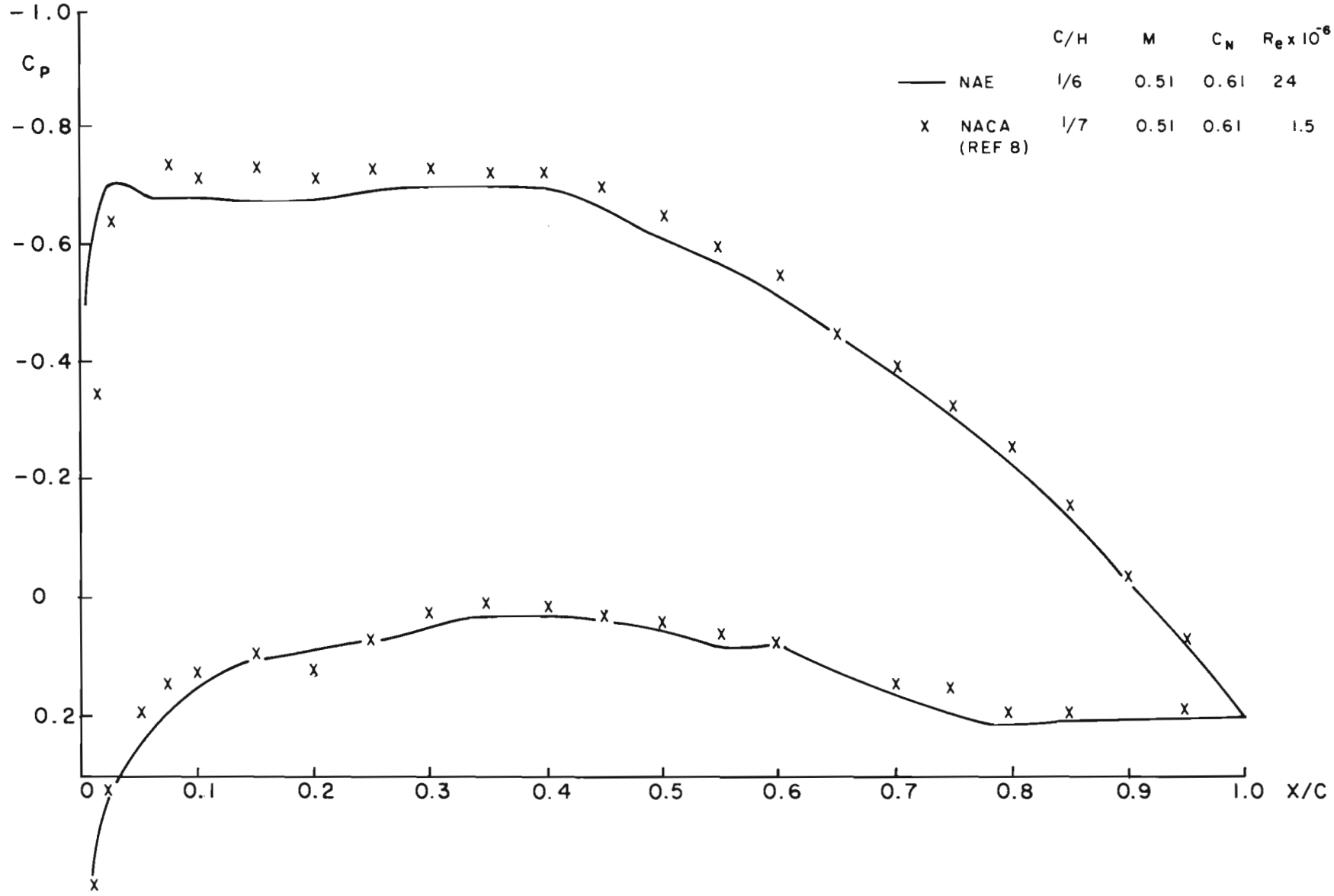

FIG.7: NAE AND NACA SUBCRITICAL PRESSURE DISTRIBUTIONS FOR THE NACA 64A410 AIRFOIL

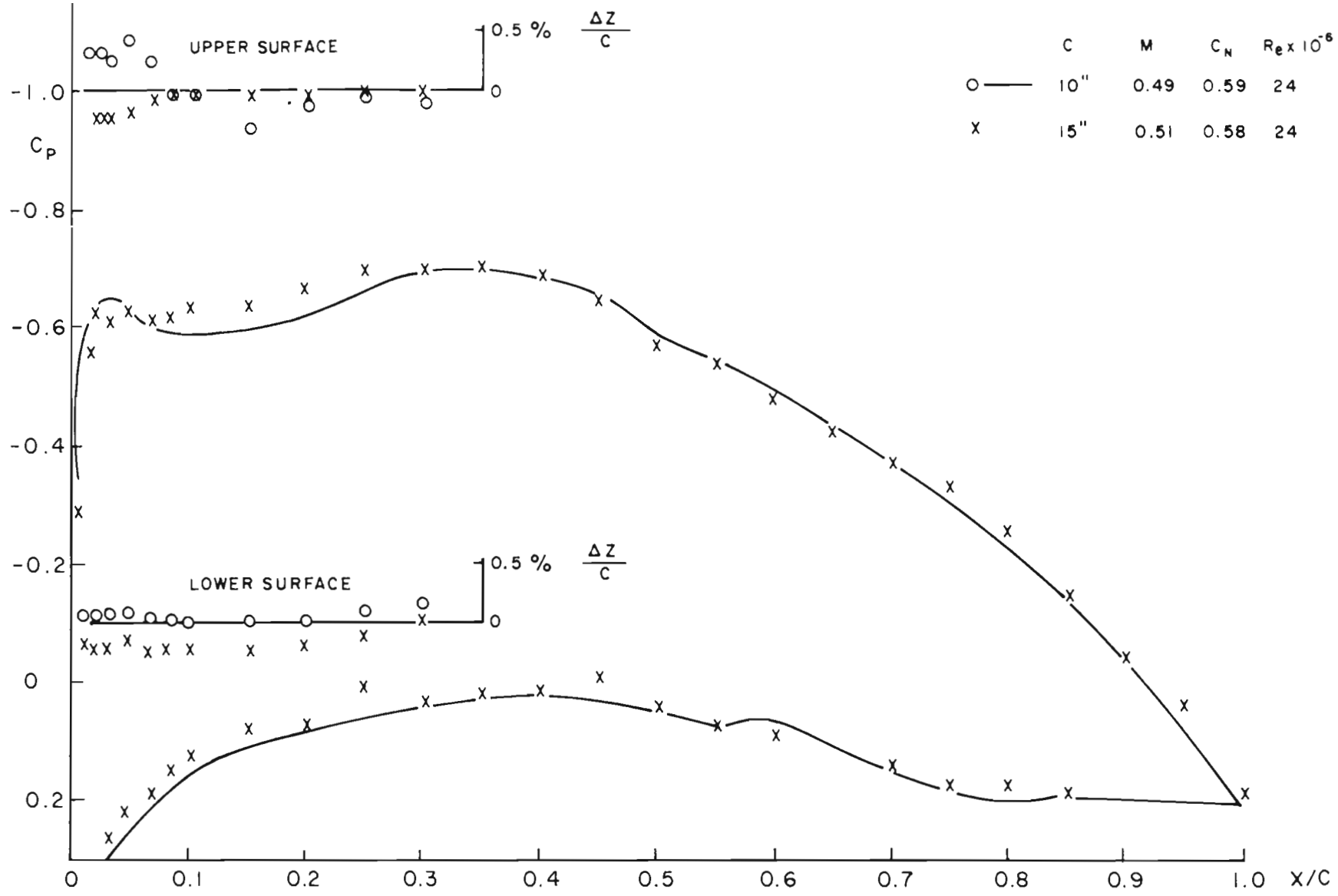

FIG.8: SUBCRITICAL PRESSURE DISTRIBUTIONS AND PROFILE ERRORS FOR THE NAE 10-INCH AND 15-INCH CHORD MODELS OF THE NACA 64A410 AIRFOIL SECTION

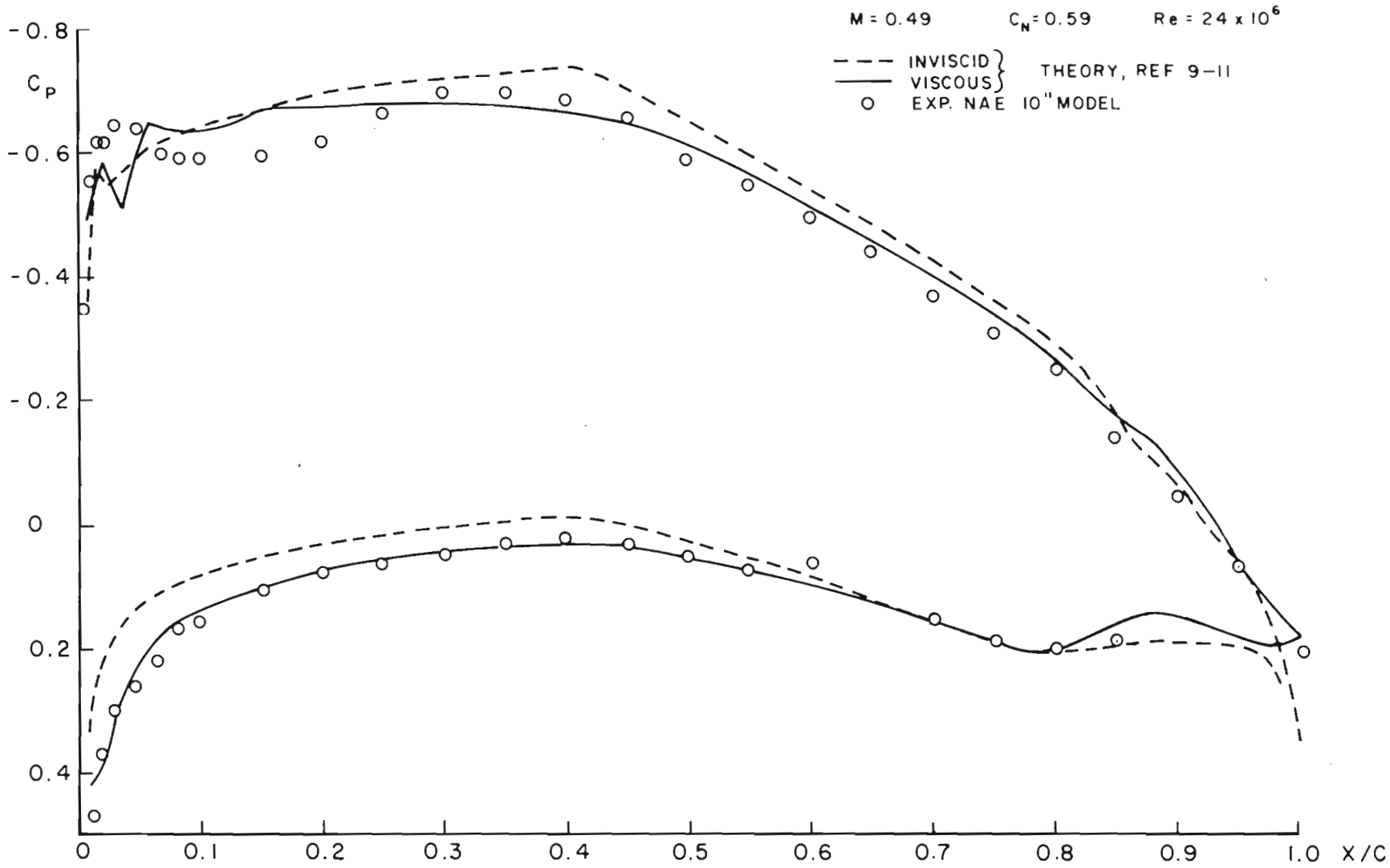

FIG.9: EXPERIMENTAL AND THEORETICAL SUBCRITICAL PRESSURE DISTRIBUTIONS FOR THE NACA 64A410 AIRFOIL

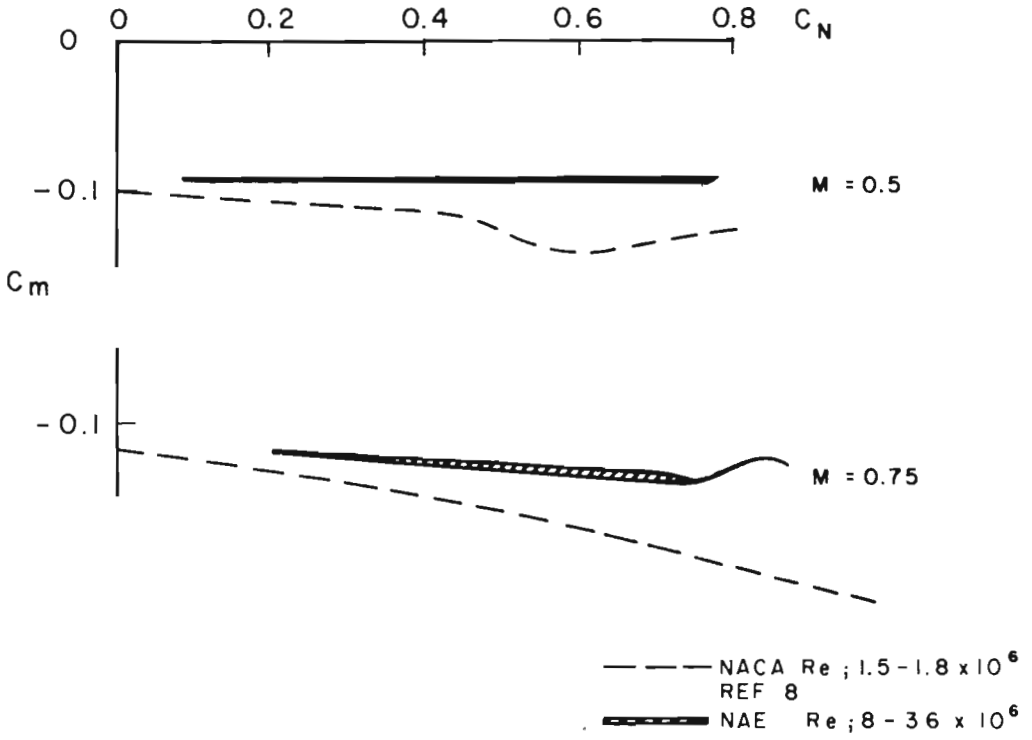

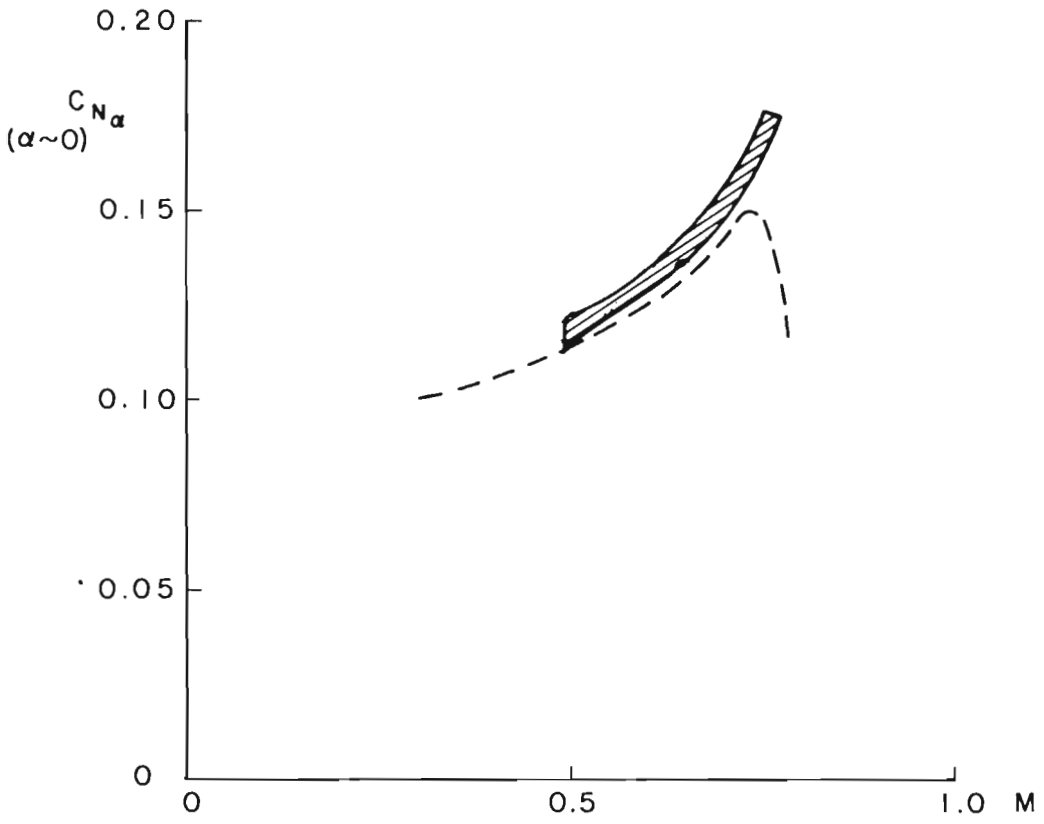

FIG.10: NACA AND NAE EXPERIMENTAL DATA FOR THE NACA 64A410 AIRFOIL SECTION

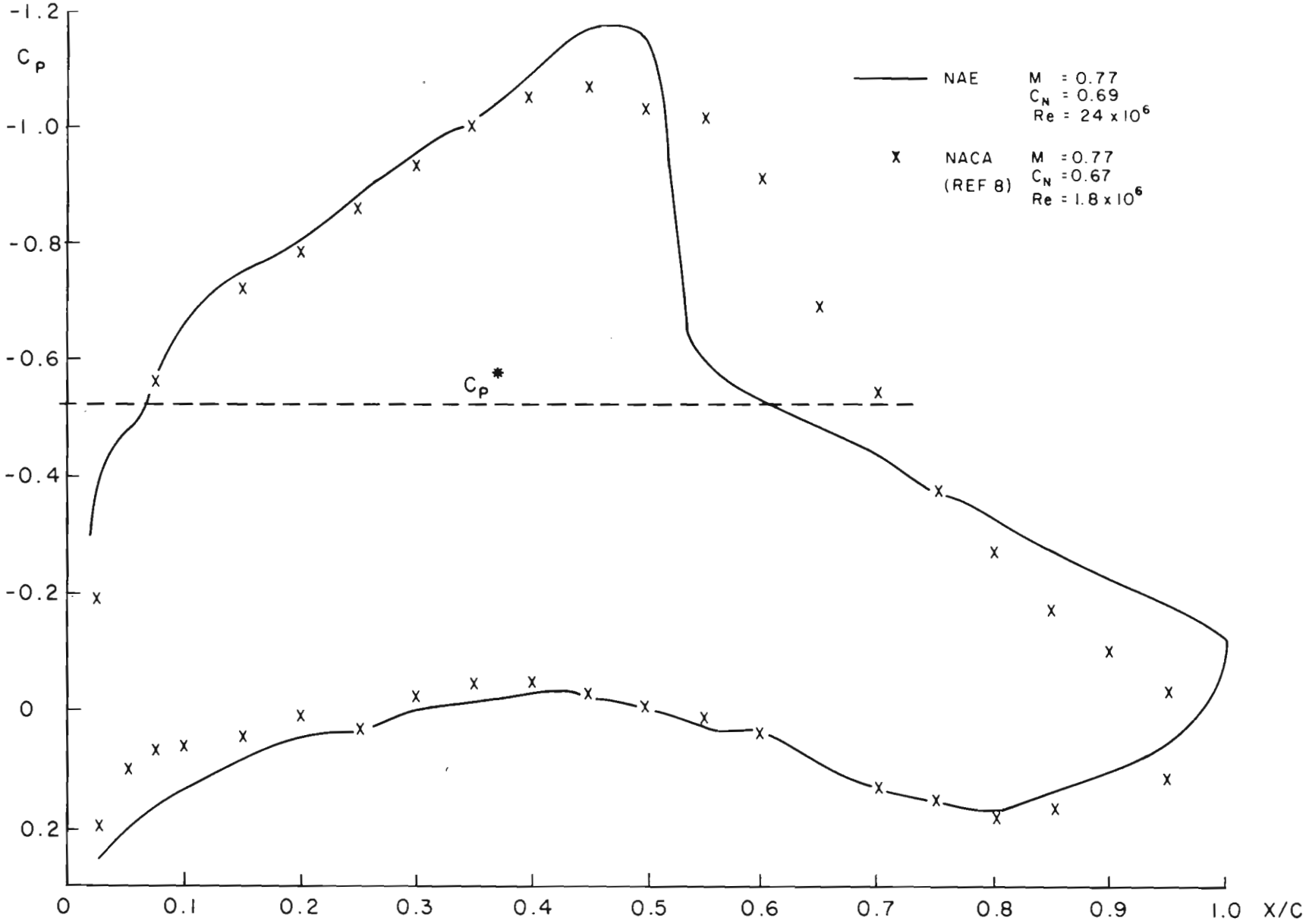

FIG.11: EFFECT OF REYNOLDS NUMBER ON SUPERCRITICAL PRESSURE DISTRIBUTION FOR NACA 64A410 AIRFOIL

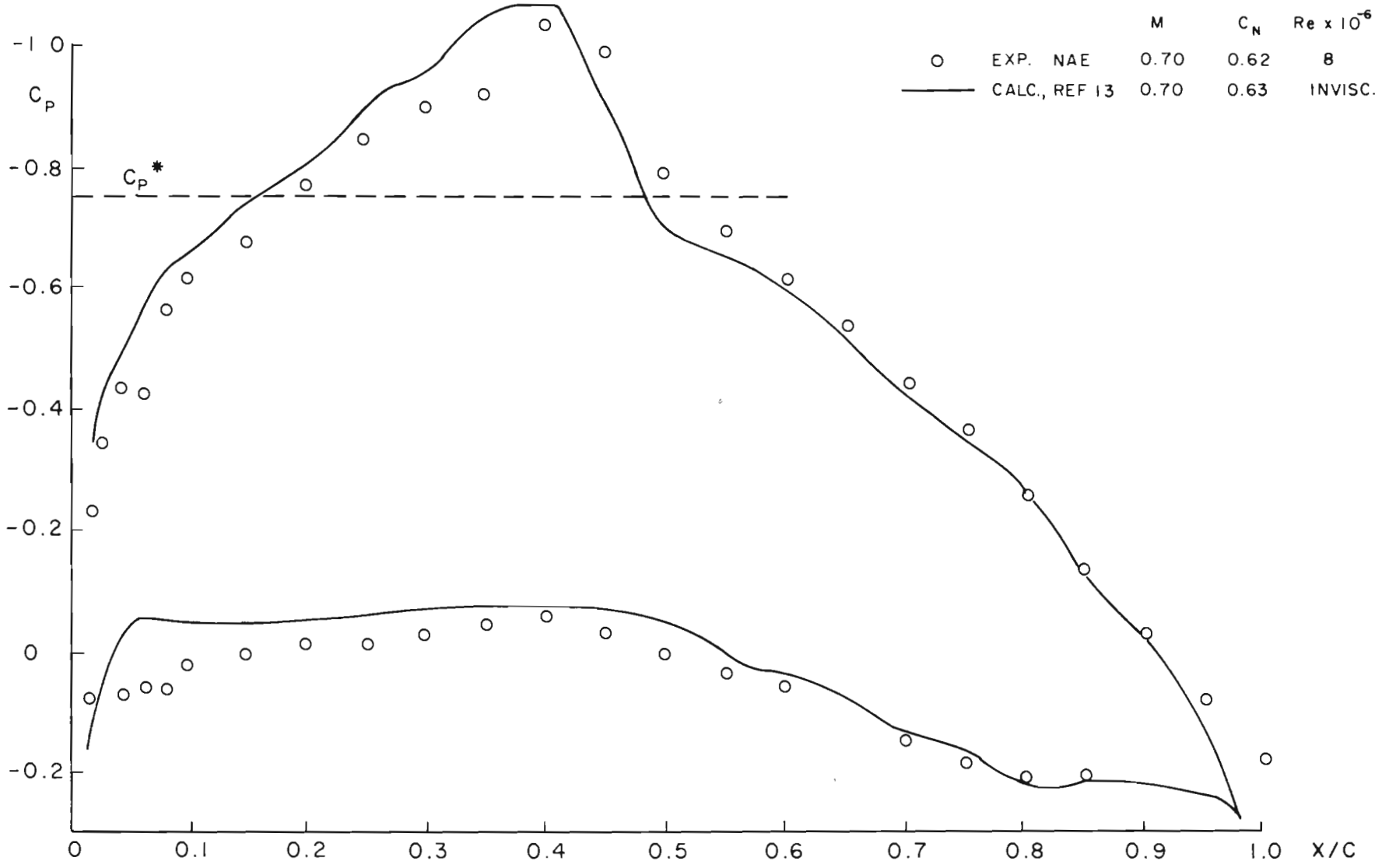

FIG. 12 a: EXPERIMENTAL AND CALCULATED SUPERCRITICAL PRESSURE DISTRIBUTIONS FOR NACA 64A410 AIRFOIL

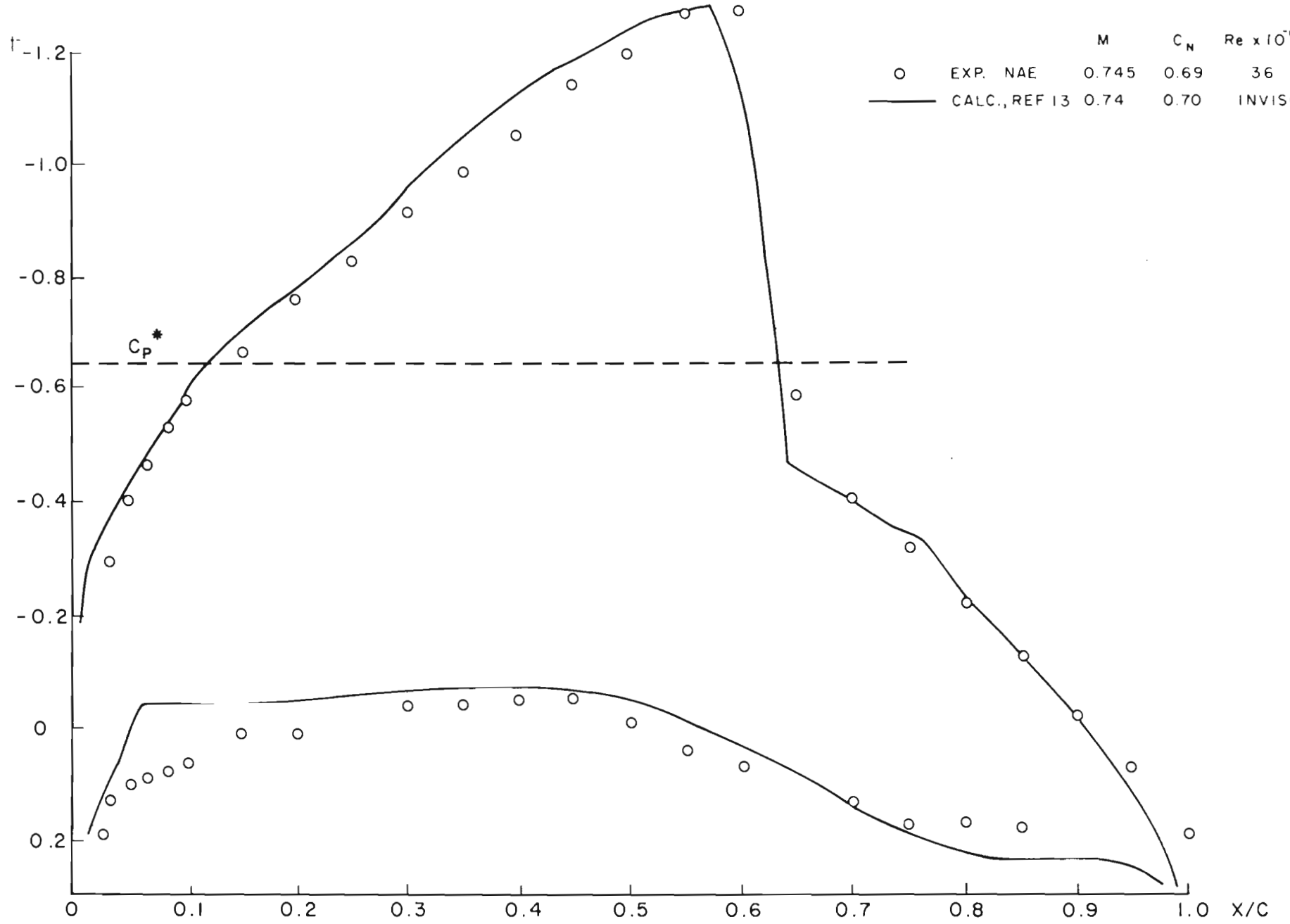

FIG.12b: EXPERIMENTAL AND CALCULATED SUPERCRITICAL PRESSURE DISTRIBUTIONS FOR NACA 64A410 AIRFOIL

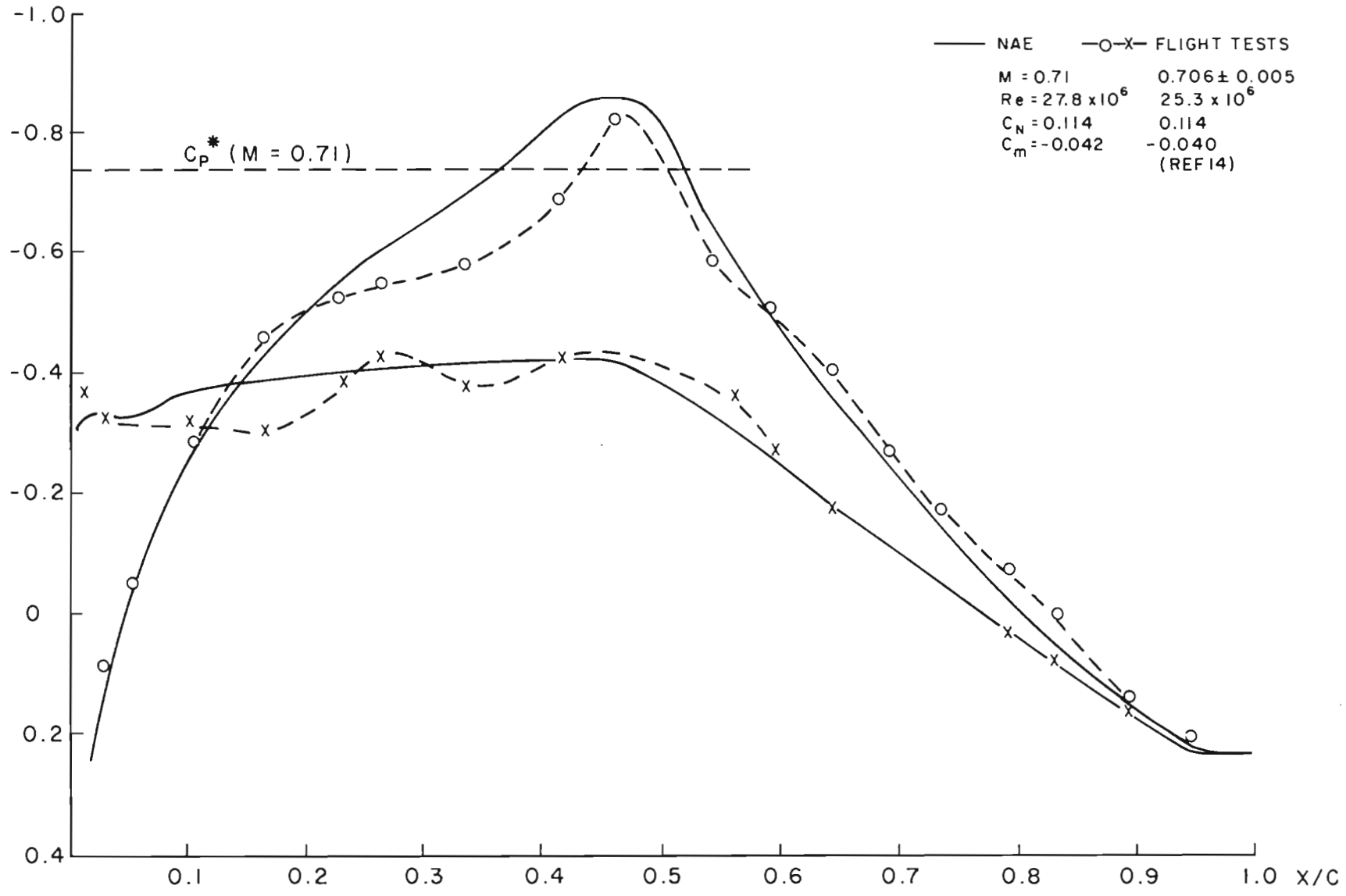

FIG. 13a: PRESSURE DISTRIBUTIONS FROM NACA FLIGHT TESTS AND NAE WIND TUNNEL TESTS FOR NACA 65,-213 AIRFOIL

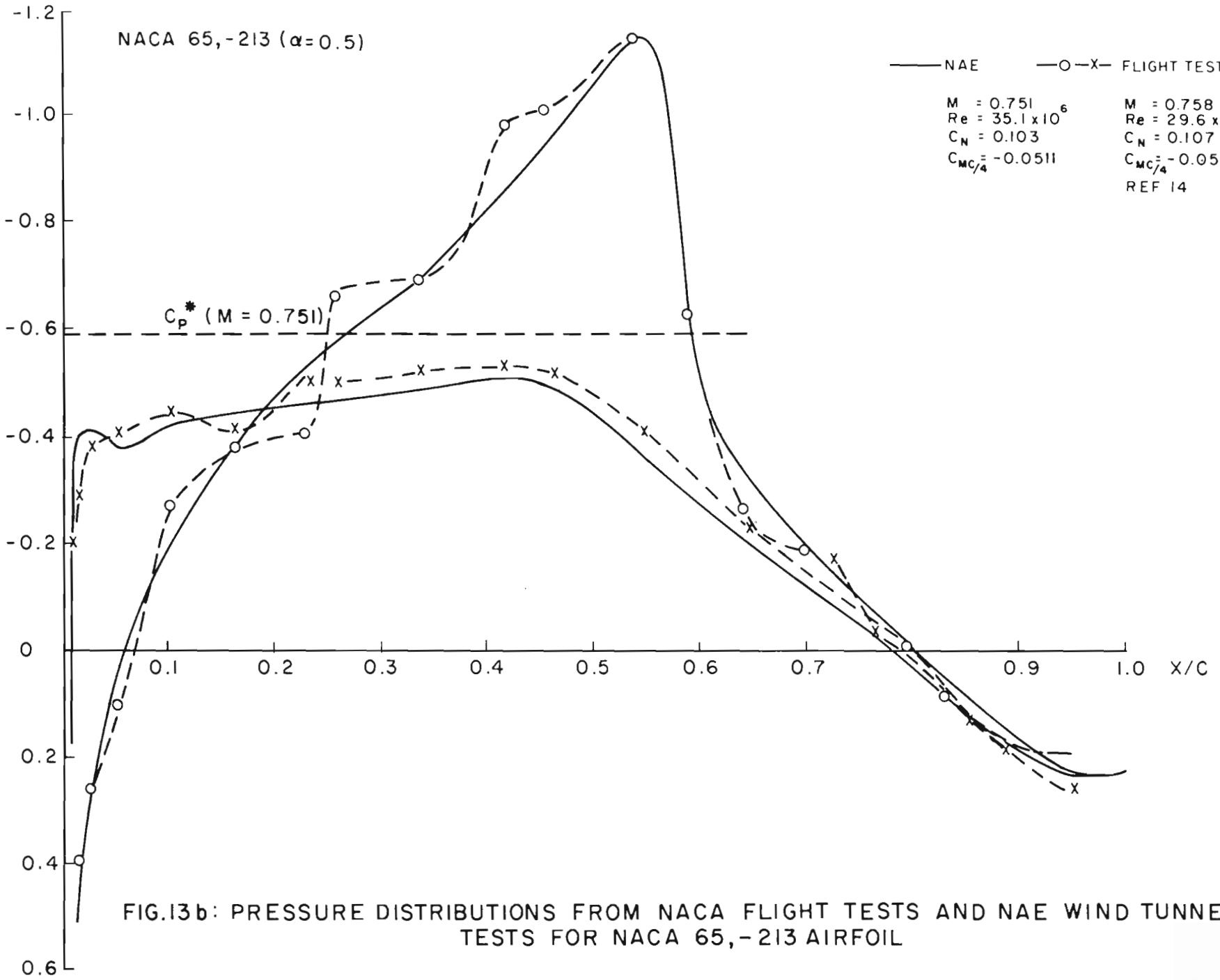

FIG.13b: PRESSURE DISTRIBUTIONS FROM NACA FLIGHT TESTS AND NAE WIND TUNNEL TESTS FOR NACA 65,-213 AIRFOIL

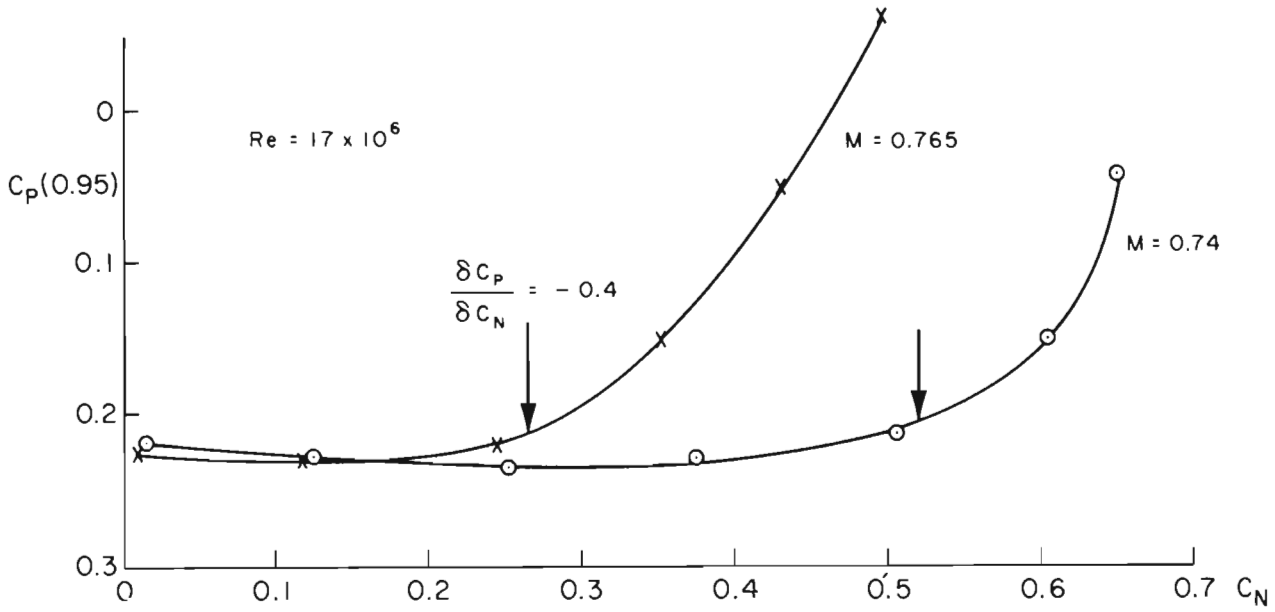

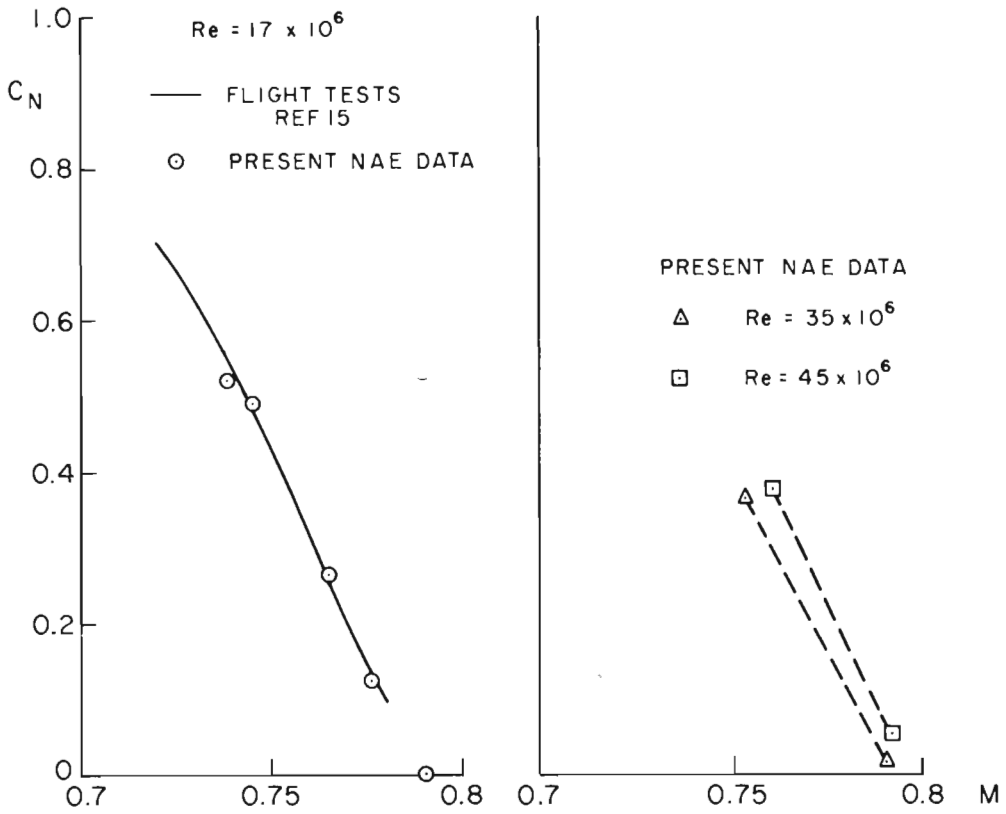

FIG. 14 : BUFFET BOUNDARIES FOR NACA 65, − 213 AIRFOIL SECTION, FLIGHT AND NAE WIND TUNNEL TESTS

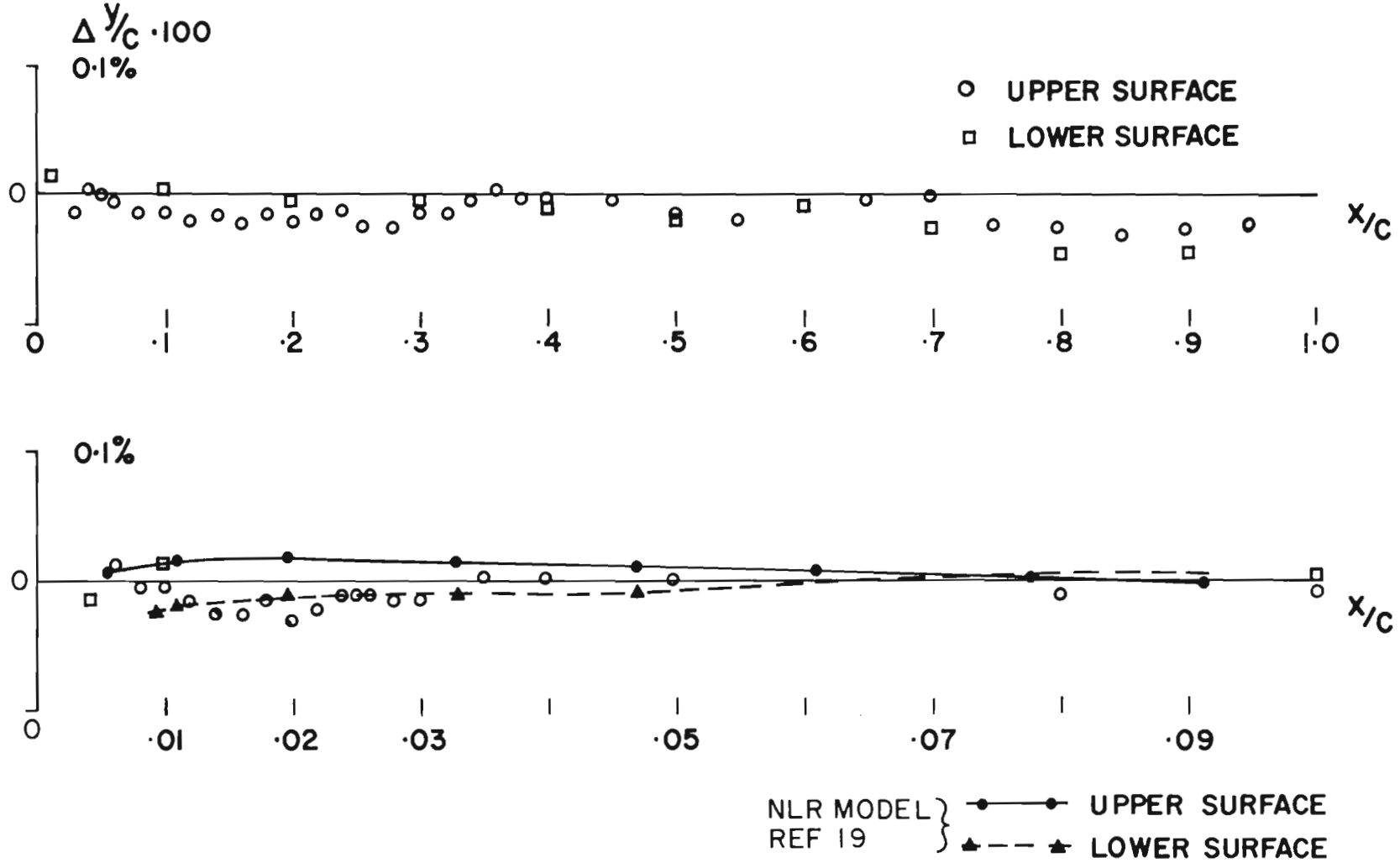

FIG. 15: DISCREPANCIES BETWEEN ACTUAL AND THEORETICAL MODEL THICKNESS CO-ORDINATES FOR NLR SHOCKLESS SYMMETRICAL AIRFOIL

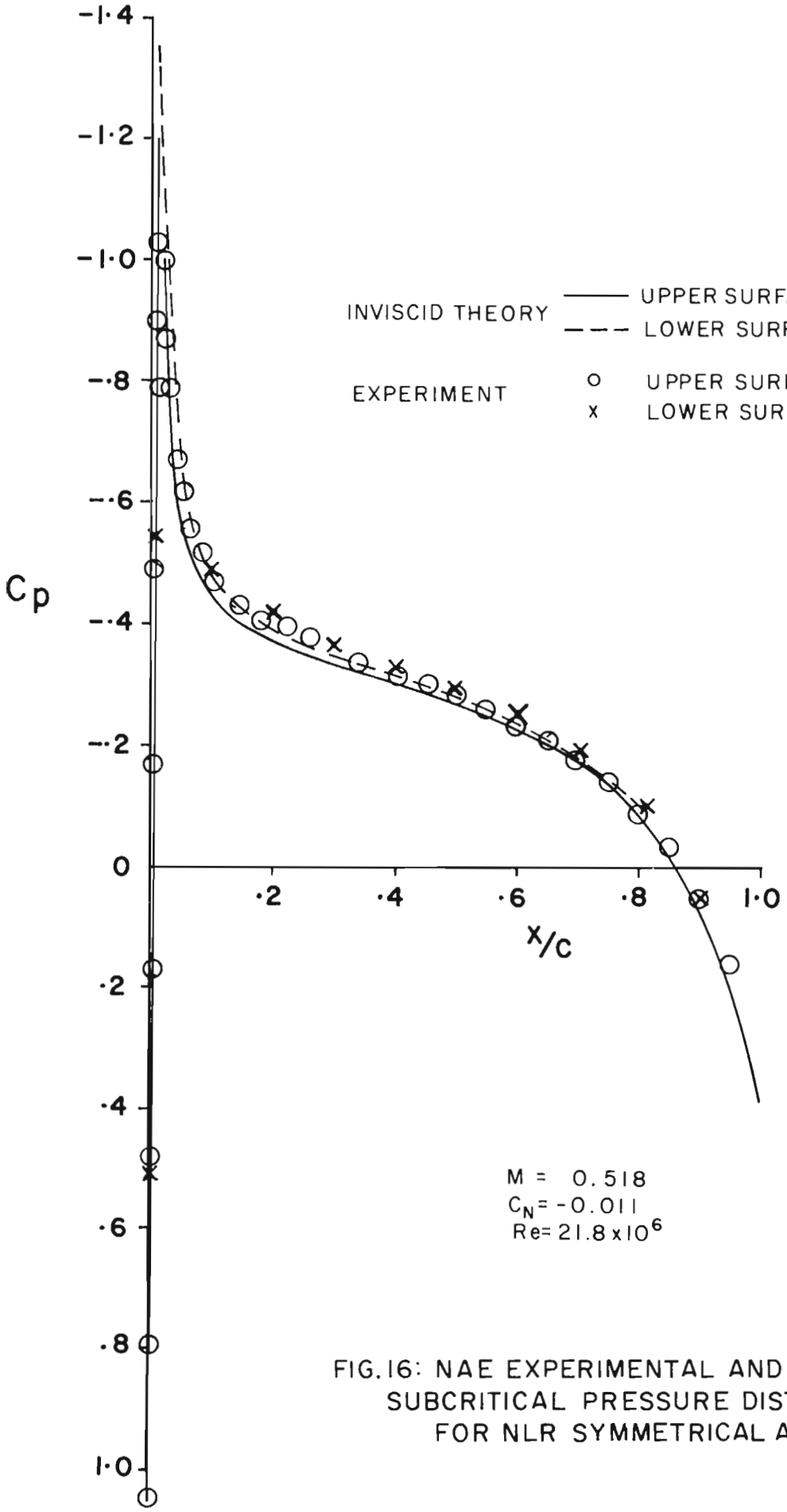

FIG. 16: NAE EXPERIMENTAL AND CALCULATED SUBCRITICAL PRESSURE DISTRIBUTION FOR NLR SYMMETRICAL AIRFOIL

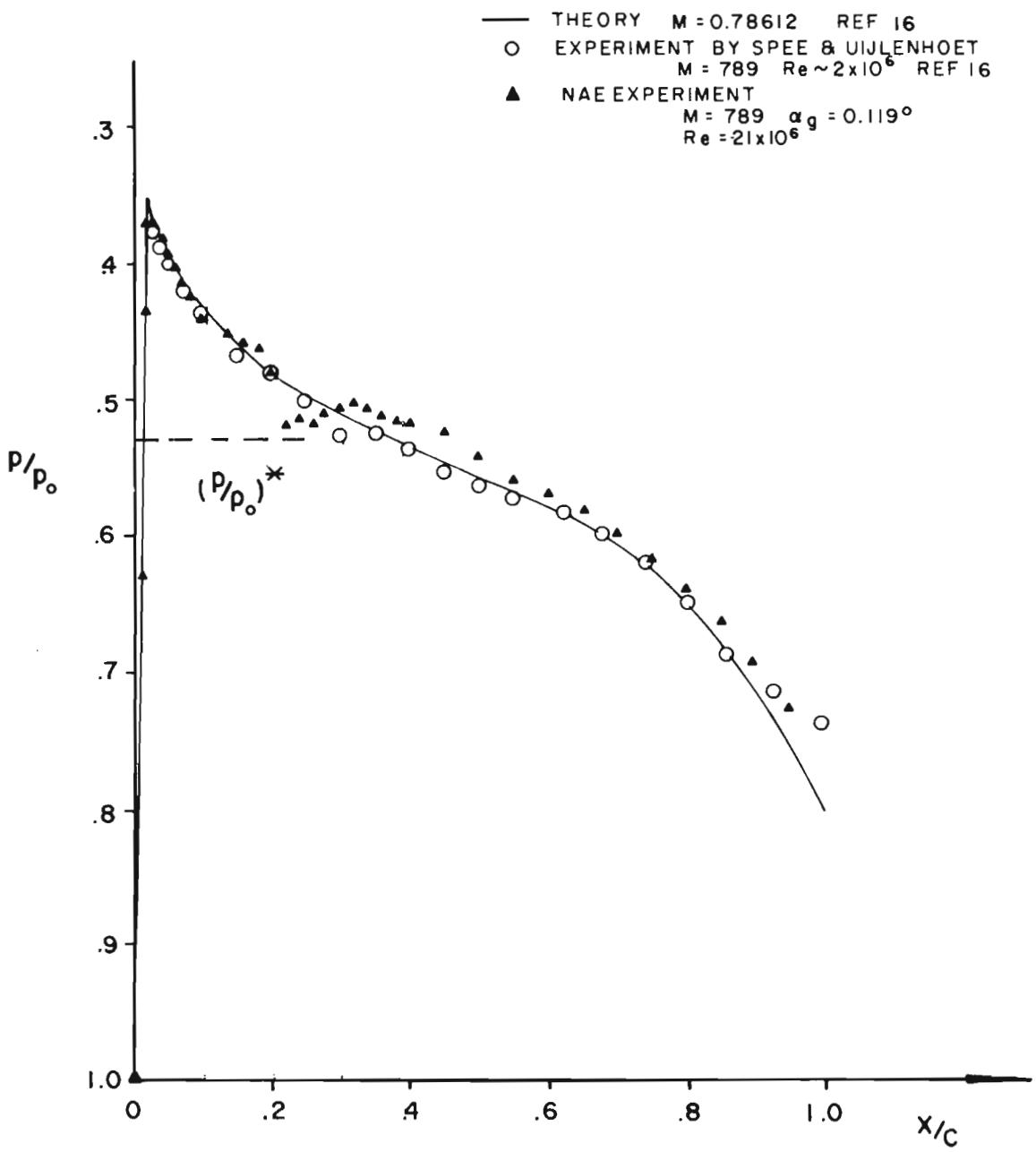

FIG.17: NAE AND NLR EXPERIMENTAL PRESSURE DISTRIBUTIONS FOR THE DESIGN CASE FOR THE NLR SYMMETRICAL AIRFOIL

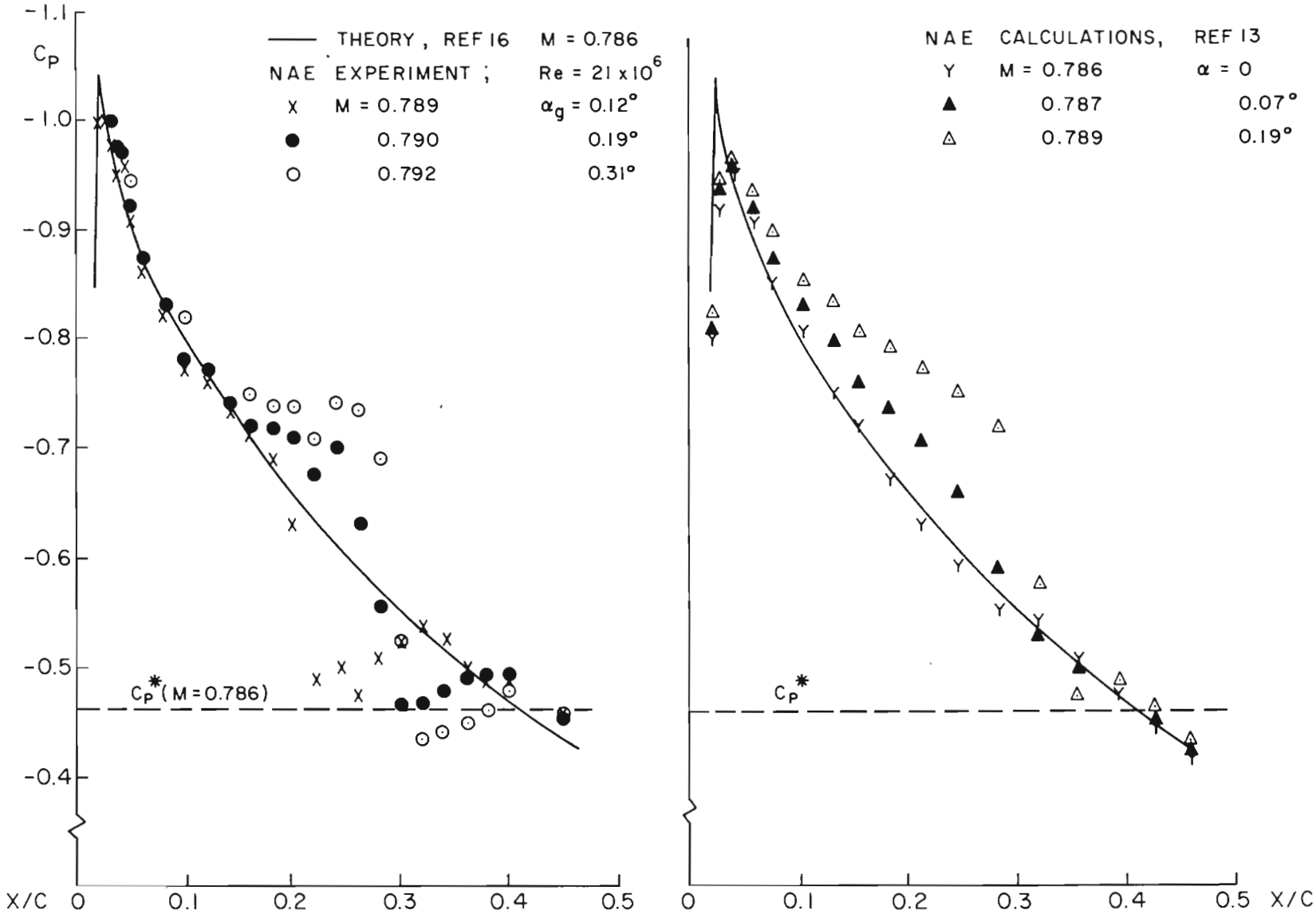

FIG.18 : SENSITIVINESS OF PRESSURE DISTRIBUTION TO SMALL CHANGES IN FLOW PARAMETERS FOR N L R SYMMETRICAL AIRFOIL NEAR DESIGN MACH NUMBER

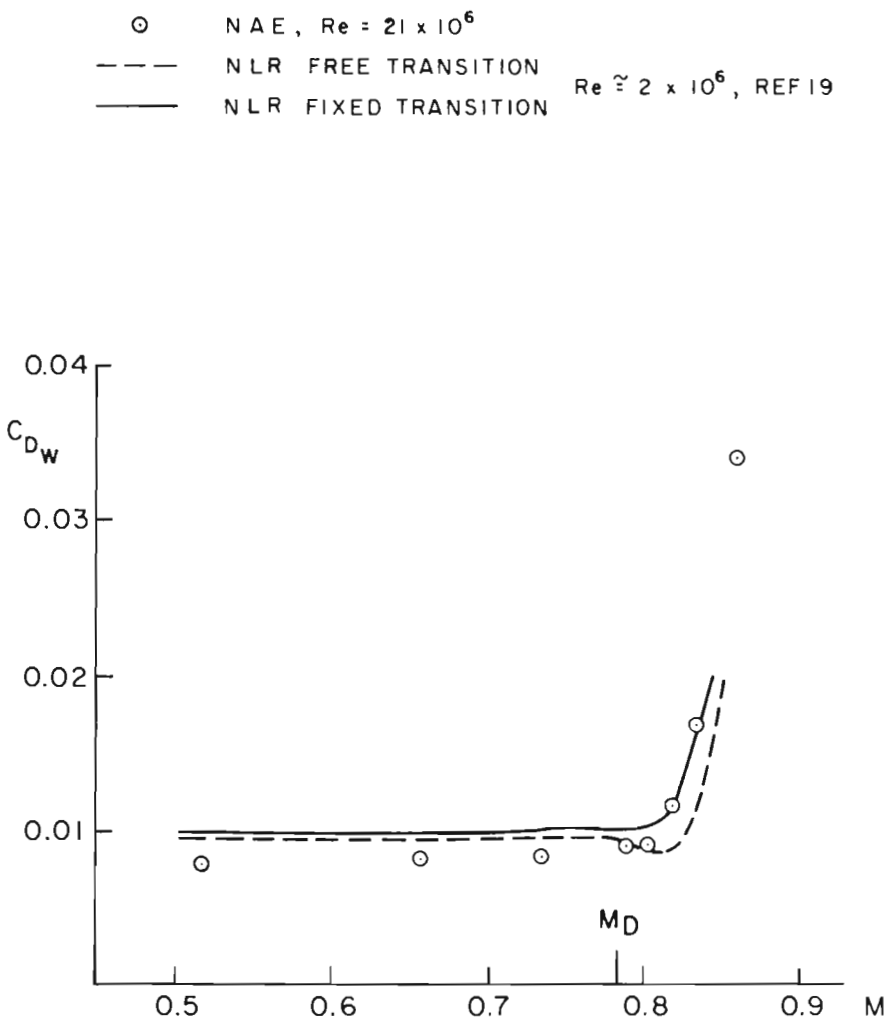

FIG. 19 : NAE AND NLR WAKE DRAG DATA FOR NLR SYMMETRICAL AIRFOIL

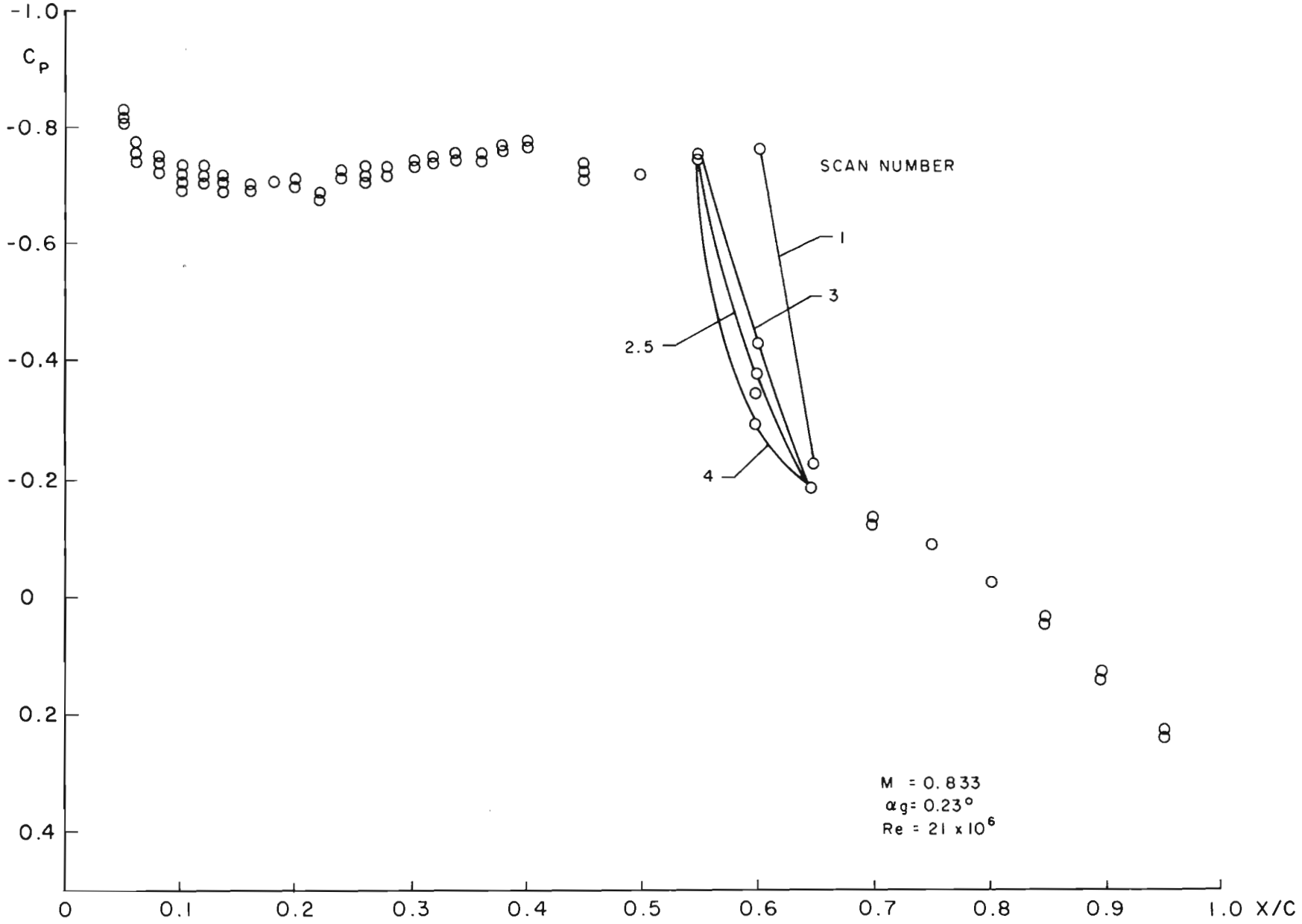

FIG.20: EXAMPLE OF PRESSURE FLUCTUATIONS IN SUPERCRITICAL FLOW FOR NLR SYMMETRICAL AIRFOIL

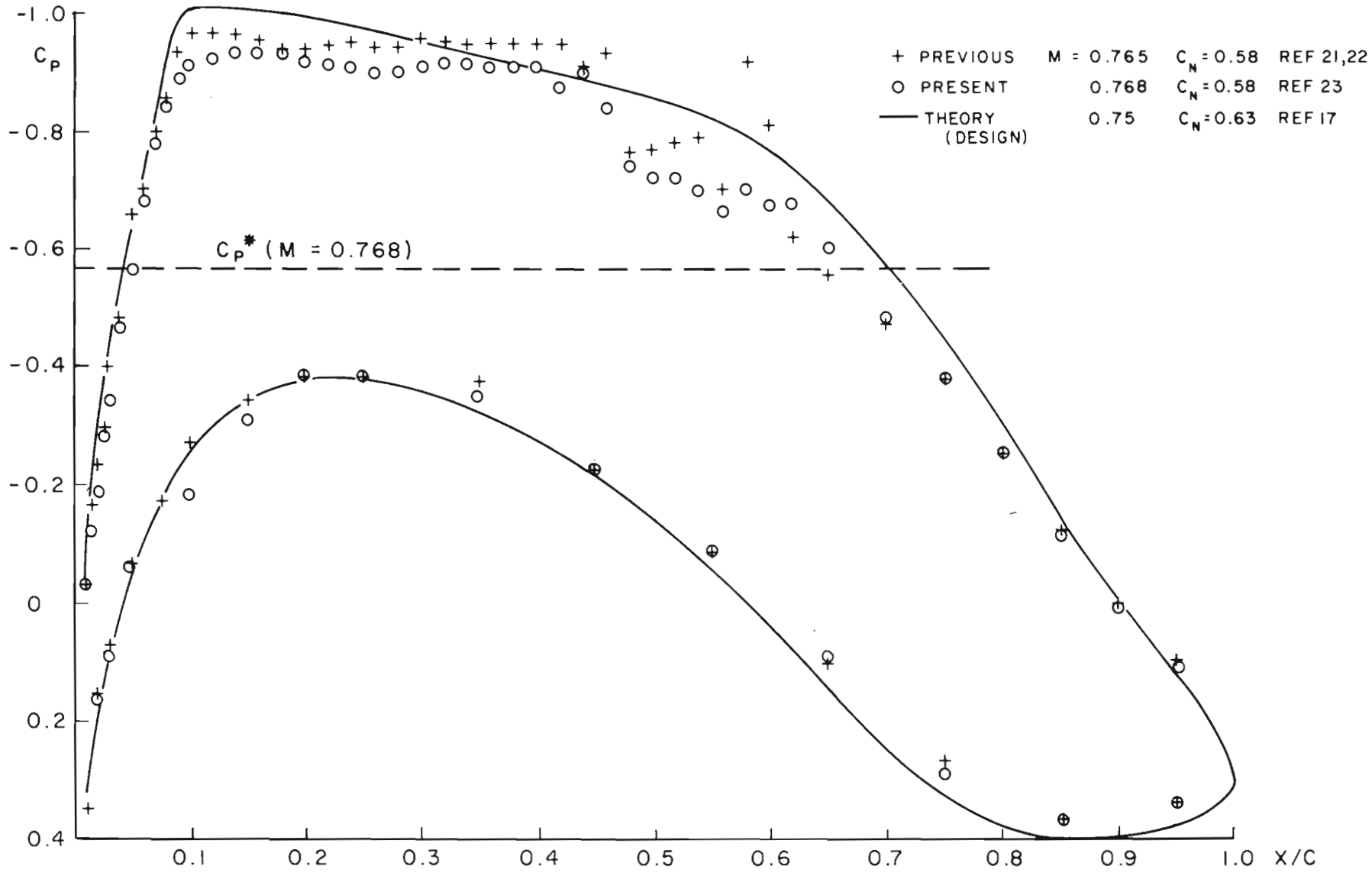

FIG. 21 : PREVIOUS AND PRESENT DATA FOR SHOCKLESS LIFTING AIRFOIL AT NEAR DESIGN CONDITIONS FOR $Re = 21 \times 10^6$

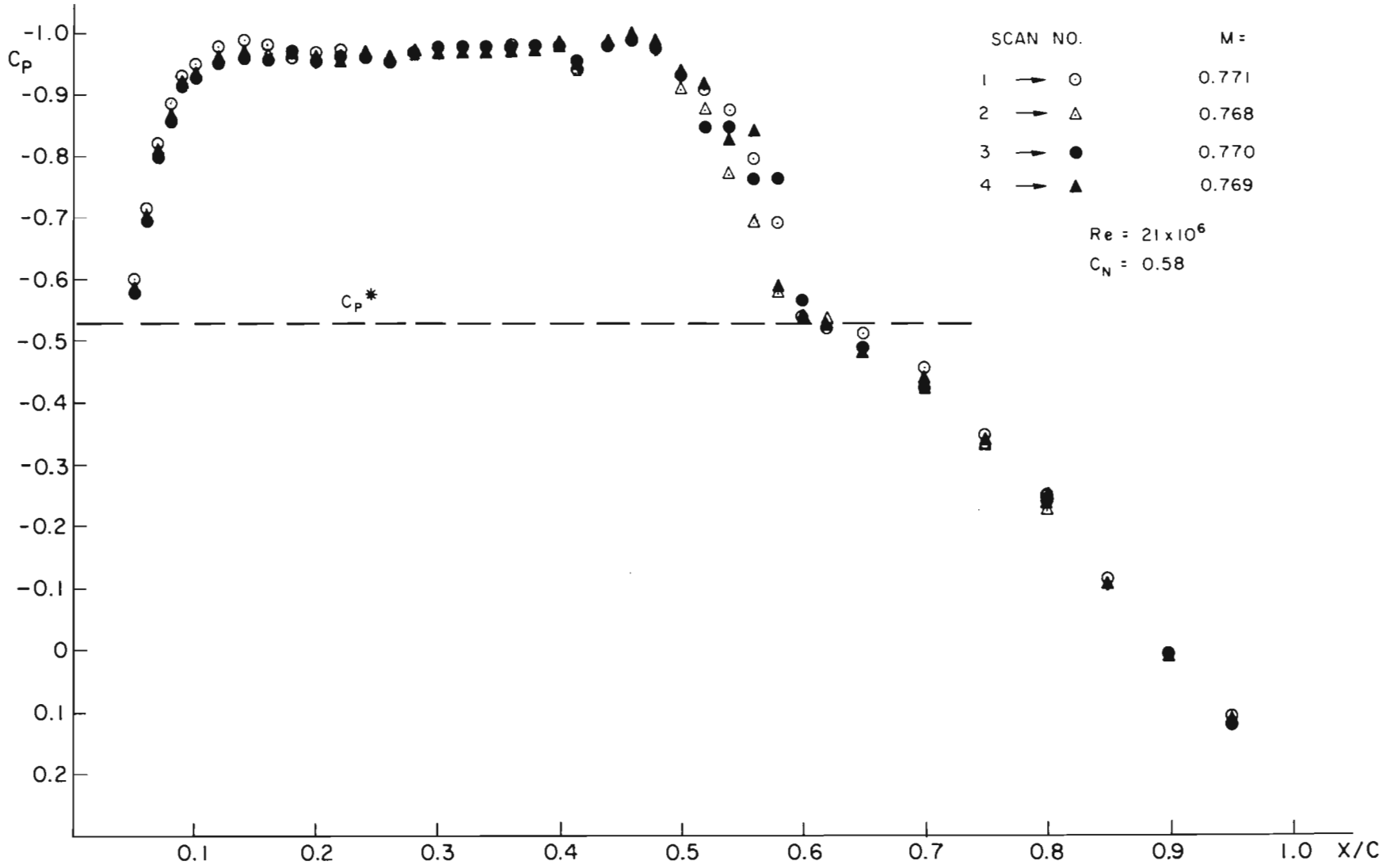

FIG. 22: PRESSURE FLUCTUATIONS FOR SHOCKLESS LIFTING AIRFOIL NEAR DESIGN CONDITIONS

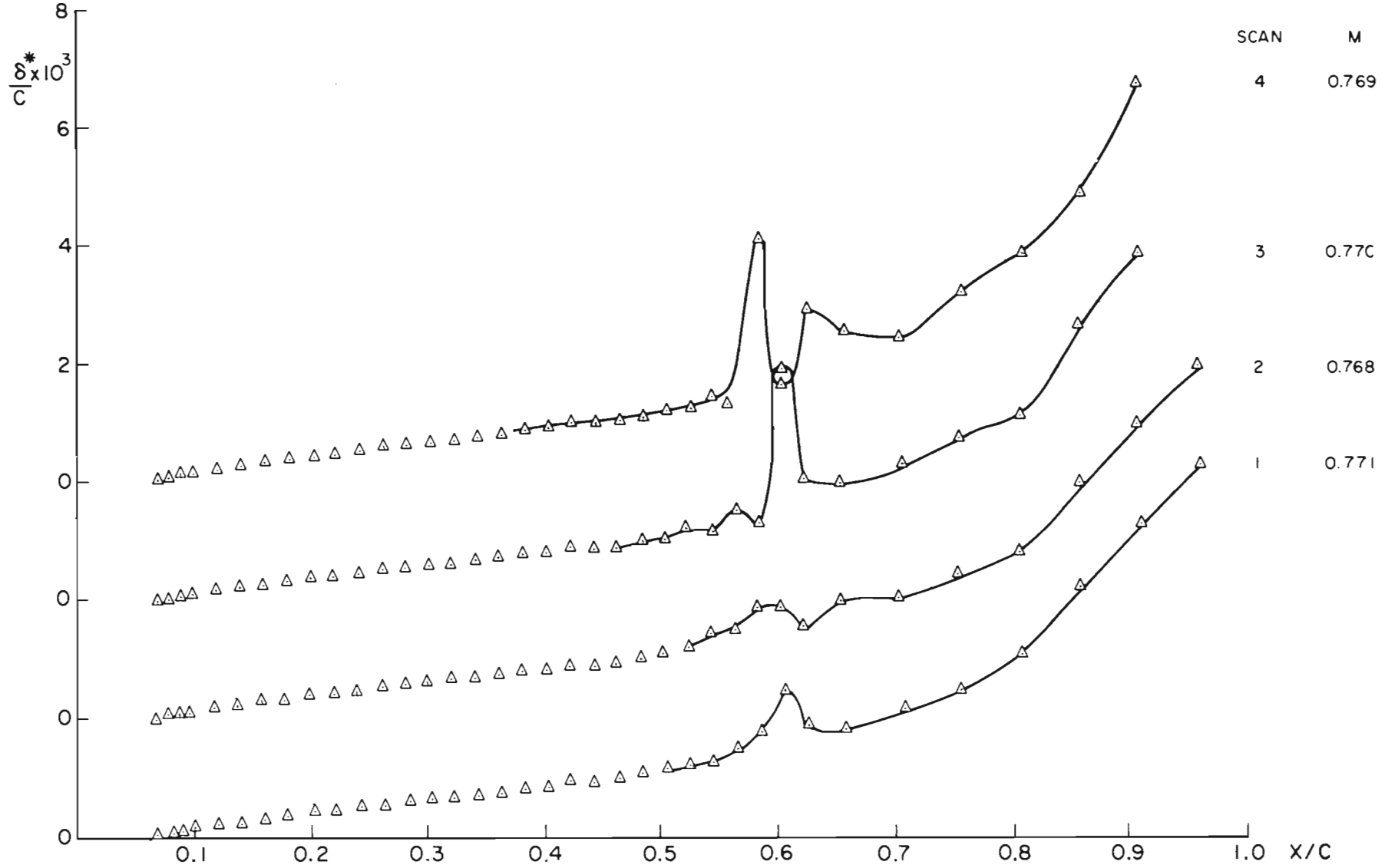

FIG. 23 : RESULTS OF BOUNDARY LAYER CALCULATIONS FOR SHOCKLESS LIFTING AIRFOIL NEAR DESIGN CONDITIONS FOR $Re = 21 \times 10^6$

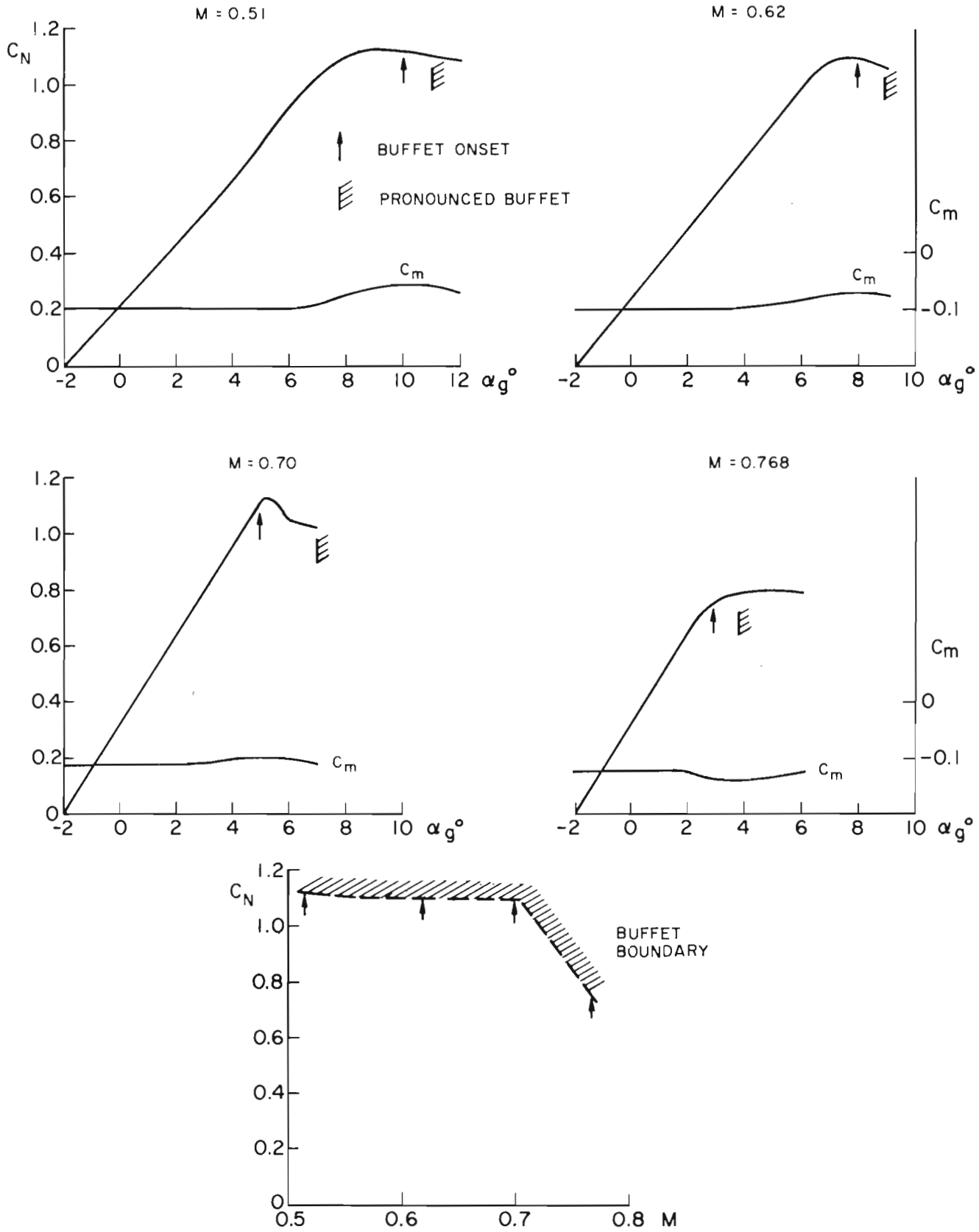

FIG.24: C_N vs α AND BUFFET BOUNDARIES FOR SHOCKLESS LIFTING AIRFOIL AT Re = 21 x 10^6

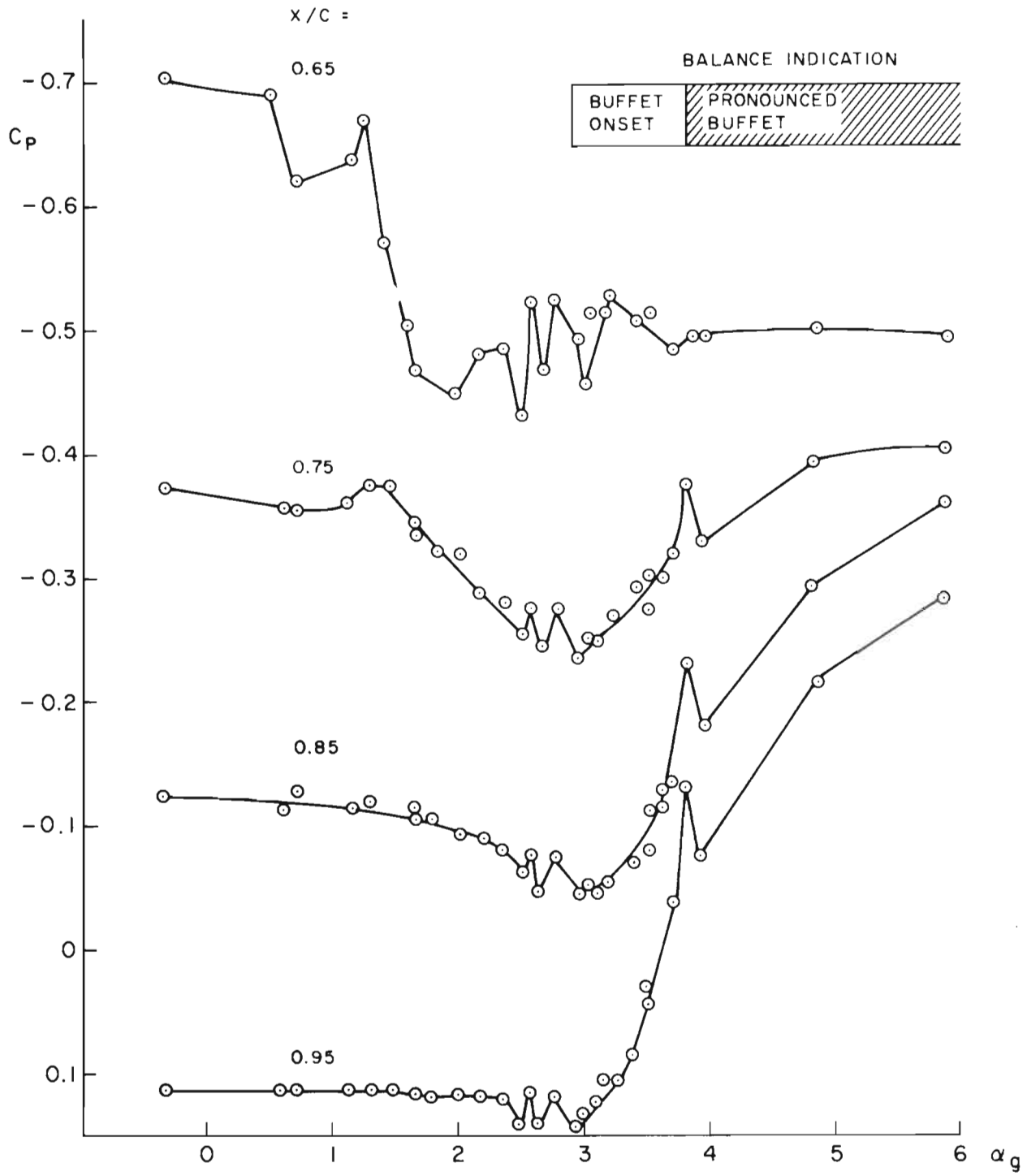

FIG. 25 : C_P vs α FOR BUFFET INDICATION FOR SHOCKLESS LIFTING AERFOI
AT M = 0.768 ± 0.002 AND Re = 21 x 10^6

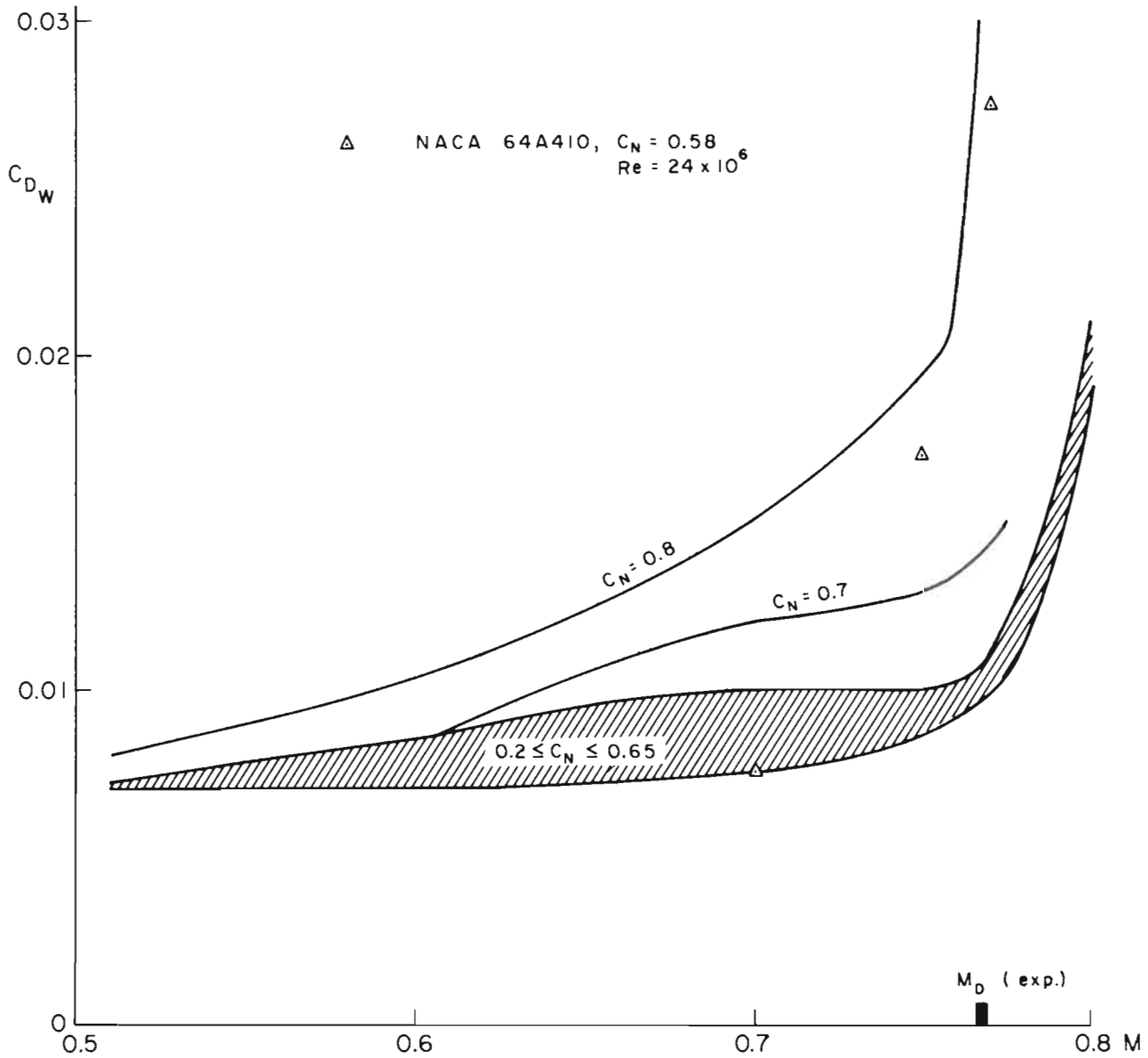

FIG. 26 : C_{D_W} vs M FOR SHOCKLESS LIFTING AIRFOIL AT VARIOUS C_N FOR Re = 21 x 10^6

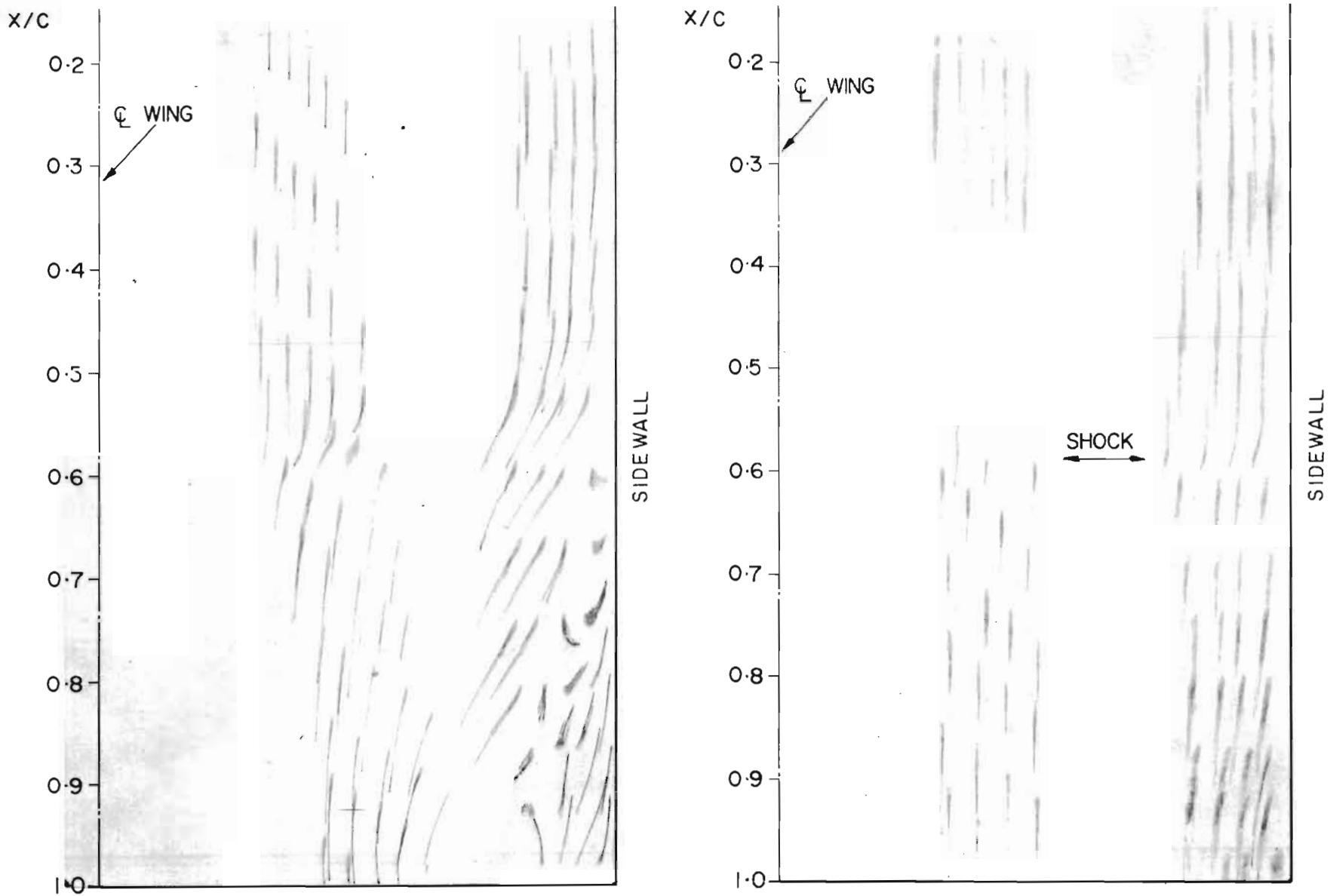

FIG. 27: EFFECT OF SIDEWALL SUCTION ON SURFACE FLOW; NACA 64A410 15-INCH CHORD MODEL AT M = 0.75, $\alpha_g \simeq 3°$

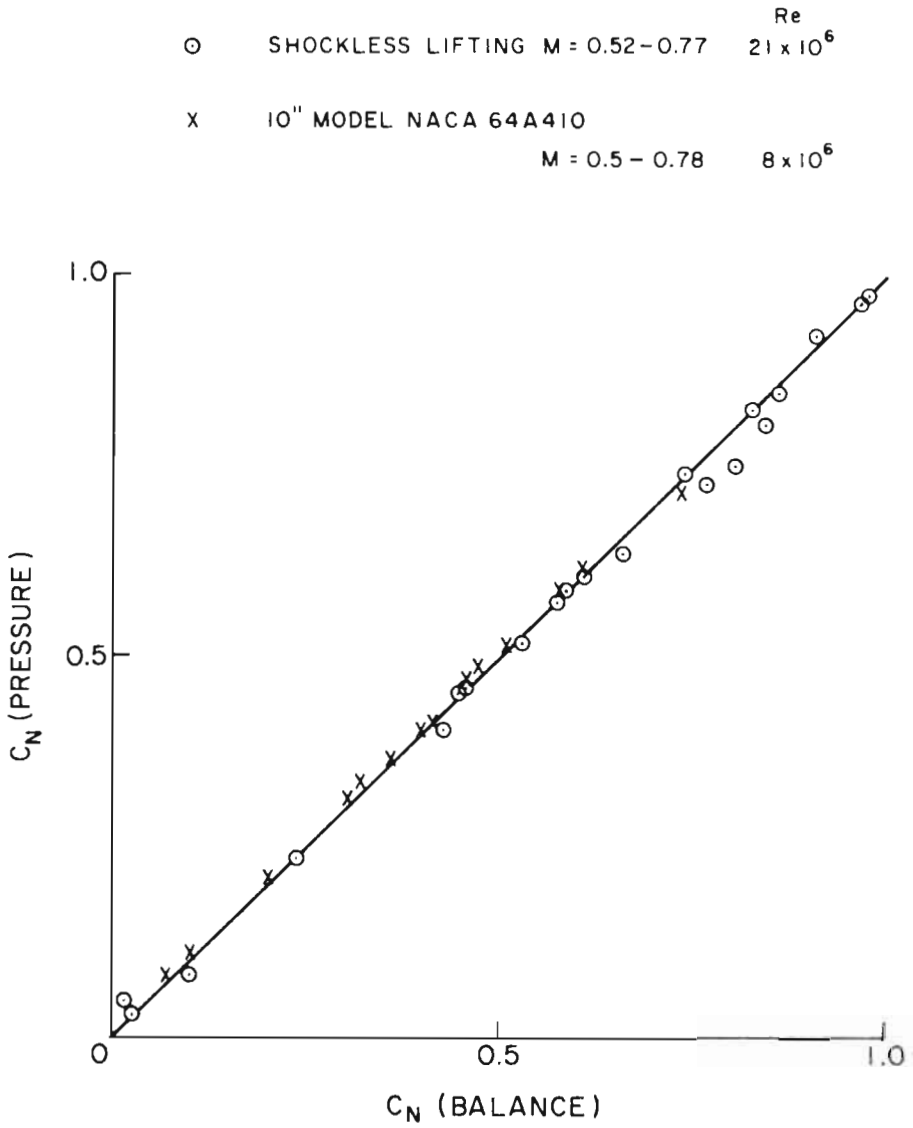

FIG.28 : CORRESPONDENCE BETWEEN C_N(PRESSURE) AND C_N(BALANCE) IN NAE EXPERIMENTS

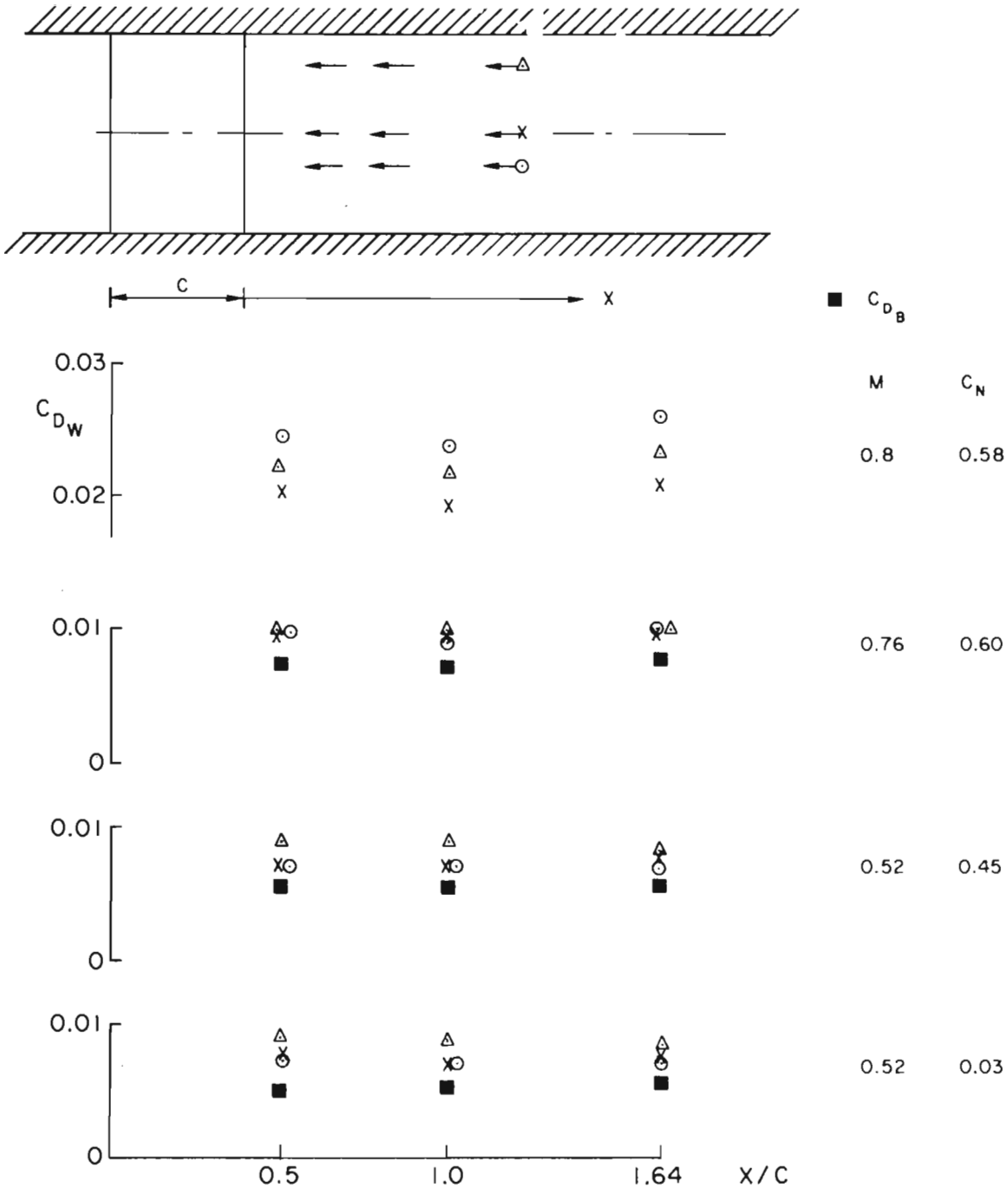

FIG.29 : WAKE DRAG vs DISTANCE DOWNSTREAM OF TRAILING EDGE AND COMPARISON WITH BALANCE DRAG FOR SHOCKLESS LIFTING AIRFOIL AT $Re = 21 \times 10^6$